Radio Echo Studies of the Moon at 23 cm Wavelength

J. V. Evans and T. Hagfors

Lincoln Laboratory,* Massachusetts Institute of Technology

1 December 1965

*Operated with support from the U. S. National Aeronautics and Space Administration.

DS-2826

Radio Echo Studies of the Moon at 23 cm. Wavelength

J. V. Evans and T. Hagfors
Lincoln Laboratory,* Massachusetts Institute of Technology

ABSTRACT

Short pulse radio reflection studies have been made to determine the average scattering behavior of the lunar surface at a wavelength of 23 cm. The intensities of both the polarized (expected) and depolarized components of the return have been measured. A precise determination of the total radar cross section of the moon σ_o using the Lincoln Calibration Sphere (LCS) satellite as a comparison standard yielded the result $\sigma_o = 0.065 \pm 0.008$ times the physical cross section (πa^2). The observations reported here are compared with earlier measurements at 68 and 3.6 cm wavelength. It is concluded that though the smoother parts of the moon's surface scatter in much the same fashion at 23 cm wavelength as at 68 cm wavelength, there appears to be an increase in the amount of surface covered with structure comparable in size to the wavelength. Attempts to account for the scattering theoretically are reviewed, and it is shown that, as yet, no complete understanding has been achieved of the reflection properties of lunar and planetary surfaces containing structure both much larger than and comparable in size to the exploring wavelength. It is believed, however, that the mean surface slope of 10° is applicable to elements of the surface of the order of five to ten wavelengths across, and is therefore the slope that might be encountered by a landing vehicle.

*Operated with support from the U.S. National Aeronautics and Space Administration.

Introduction

As a result of previous studies of the moon it has been established that at meter wavelengths the reflections arise predominantly from a small central region on the lunar disk where the surface is nearly normal to the direction of incidence and reflection. The regions nearer to the limbs appear approximately uniformly bright, and contribute only a small fraction of the total reflected power (Evans and Pettengill, 1963a). As the wavelength is reduced, the bright central region becomes less intense with respect to its surroundings and expands in size. Also the fraction of the power attributable to the uniformly bright region increases, and at a wavelength of about 2 cm probably accounts for half the total power (Evans and Pettengill, 1963b). At 8.6 mm the surface appears almost uniformly bright (Lynn et al, 1963) – as it does optically at full moon (Markov, 1948). For a recent review the reader is referred to Evans (1965).

These results have been interpreted as indicating that on a scale of a meter the surface is largely smooth and undulating, with a mean surface slope that is related to the size of the central bright region. It is thought that the limb region appears almost uniformly bright because for large angles between the ray and surface normal few plane elements are found perpendicular to the ray path, and hence small structure which can scatter into wide angles is responsible for the reflections. Thus as the exploring wavelength is shortened the mean slope appears to increase, and the amount of power contributed by the small scale structure on the surface increases also. This implies a whole spectrum of different size surface structure in which there is an increasing amount having scales on the order of the wavelength of observation with decreasing wavelength. From the Ranger pictures it seems that much of this structure must be associated with small craters whose number increase rapidly as their size is reduced (Heacock et al, 1965).

The experimental results reported by Pettengill and Henry (1962), Evans and Pettengill (1963b), Klemperer (1965) and others have stimulated a large number of attempts to deduce theoretically from these reflection properties a physical description of the surface. We review briefly this work and show that the theory may be regarded as satisfactory only for long wavelengths, where the

surface may realistically be assumed to be locally smooth. The fact that the reflection properties change with wavelength demonstrates that this assumption is only an approximation, and one which becomes increasingly inaccurate as the wavelength is shortened.

In Section II which follows we briefly outline the nature of the earlier published measurements and indicate why additional ones are desirable. Section III describes the apparatus and observing procedure, Section IV the new results and Section V their interpretation. In Section VI we discuss the relation between the radio scattering properties of the lunar or a planetary surface and the nature of the lunar terrain.

II. Previous Short Pulse Observations

Short pulse studies of the lunar surface have been made at a number of wavelengths. These measurements are, in our view, to be preferred to other types such as power spectrum measurements discussed by Evans and Pettengill (1962a) for the following reasons: – a) better resolution can be obtained by examining the distribution of echo power with respect to delay than frequency owing to the small angular rotation rate of the moon, b) there is a direct correspondence between the echo power at a given range delay t and the angle of incidence and reflection ϕ of the radio waves, and c) for practical reasons it is possible to explore the echo power over a larger dynamic range when separating the echoes with respect to range, than when resolving them in frequency.

The scattering properties of the lunar surface were previously explored over almost the full range of angles $0 < \phi < 90^\circ$ at 3.6, 68 cm and 6 m wavelength. The pulse lengths used in these measurements and also the intervals at which the echo power was sampled (Table I) differed considerably so that the resolution obtained for small ϕ was often poor. Table I lists the observations made thus far, together with the ones reported in this paper. It can be seen that prior to the present measurements the behavior in the region $\phi - 90^\circ$ had been observed only at wavelengths of 3.6, 68 and 600 cm. In addition the pulse lengths employed prevented a useful examination of the region $\phi < 10^\circ$ at all but two wavelengths, namely 10 and 68 cm. In the observations at 23 cm wavelength reported here experiments have been conducted to match the resolution achieved at 3.6 cm and

Table I

Angular Power Spectrum Studies of the Moon

Wavelength (cm)	Observer	Pulse length	Sample Interval	Range of ϕ studied	Comments
0.86	Lynn et al (1963)	2 sec.	once per pulse	$8^\circ - 60^\circ$	Angular resolution achieved using 0.07° pencil beam
3.6	Evans & Pettengill (1963b)	30 μsec	20 μsec	$5^\circ - 80^\circ$	
10	Hughes (1961)	5 μsec	20 μsec	$2.5^\circ - 14^\circ$	Sensitivity limitations prevented higher values of ϕ from being examined.
23	This paper	10 μsec	10 μsec	$2.5^\circ - 90^\circ$	
68	Evans & Pettengill (1963b)	12 μsec	10 μsec	$2.5^\circ - 90^\circ$	
600	Klemperer (1965)	100 μsec	?	$7.5^\circ - 90^\circ$	
1130	Davis and Rohlfs (1964)	250 μsec	250 μsec	$12^\circ - 48^\circ$	Echoes read from film.

68 cm wavelength and the scattering behavior has been explored over all ϕ for both the expected and depolarized components of the echo.

III. Equipment and Observing Procedure

The observations reported herein at 23 cm wavelength were made using the Lincoln Laboratory, Millstone Hill Radar located in Westford, Massachusetts (42.6°N 71.5°W). The parameters of the equipment as employed for the present set of observations are listed in Table II. During the course of the measurements the antenna was directed to point continuously at the center of the moon's disk by means of a Univac 490 digital computer or by preparing a punched paper tape which gave pointing instructions at 10 sec intervals. Checks could be made by means of a television camera aligned along the axis of the beam to confirm that the pointing was accurate. The receiver was tuned to within 0.1 c/s of expected frequency of the echo by means of a special linearly varying frequency generator, the slope of the linear frequency variation being reset at 5 minute intervals. In addition to guiding the receiver tuning in frequency to match the expected doppler shift, the variation of the position of the echo on the time-base due to the continuously changing range was compensated to within a small fraction of the pulse length. In this way samples of the echo intensity could be taken at fixed delays with respect to the echo position, and these could be averaged to obtain the mean echo power at that delay. The manner in which these range and frequency compensations are provided has been described elsewhere (Evans et al, 1965).

Following the last frequency conversion in the multiple superheterodyne receiver the signals are applied to two phase detectors, which are driven at the same reference frequency but shifted in phase by 90°. The outputs of these detectors are thus the sine and cosine components of the signal. These components are separately filtered by low-pass filters (which are matched either to 10 or 20 μsec pulses, Table II) and sampled by identical digital voltmeters. The voltmeters are commanded to take samples at equal intervals of delay. A choice of several sample frequencies is available, but most of the measurements were conducted with frequencies of 50 or 100 Kc/s. The time required for the voltmeter to make a determination is 0.25 μsec. Each voltmeter determines the

Table II

The Millstone Hill L-band Radar

Frequency	=	1295.0 Mc/s
Antenna	=	84 ft. parabola with Cassegrain feed arrangement
Antenna Gain	=	47.3 db
Polarization	=	right circular transmitted right and left circular separately received
Beamwidth	=	0.6° between half power points
Transmitter power	=	variable, 5 MW peak maximum (continuously monitored)
Pulse length	=	variable, pulses of 10, 30, 100 and 200 μsecs length were employed in these observations
Receiver bandwidth	=	100 Kc/s predetector. Postdetector filter matched to 10 μsec pulses for 10 μsec pulse transmissions, matched to 20 μsec pulses for all other transmissions. Also 8 Kc/s predetector for the observations described in Sec. IVb.
System Noise Temperature	=	$\sim 150^{\circ}$K (continuously monitored)
Overall feed-line and other losses	=	2.1 db

sign of the signal and assigns it one of 32 possible levels. The total dynamic range of the receiver system is therefore limited by these voltmeters to 30 db. The echo intensity could be explored over a wider range than this, however, by raising the transmitter power and repeating the measurements at different signal-to-noise levels. The samples obtained in this fashion were recorded digitally on magnetic tape for later computer processing. In the simplest form of processing the pair of samples corresponding to a given range delay are squared and added to yield the echo power at that delay. This sum is then added to all other sums for that delay to yield an average for the echo power at that delay. It was also possible to receive both orthogonal components of the reflected signals simultaneously and sample and store the voltages corresponding to the two signals. In this way the polarization of the reflected signals (Sec. IVb) could be explored.

IVa. Results for the Polarized Component

In this measurement a circularly polarized wave of one sense was transmitted and the opposite (i.e., the expected sense) was received. In order to explore the echo power P(t) over the complete radar depth of the moon (11.6 msec) observations conducted with a variety of pulse lengths were carried out. The echo power was established for the region of delays 0-700 μsecs using a pulse 10 μsecs long and a sampling interval of 10 μsec, together with observations in which 30 μsec pulses with a 20 μsec sample interval were used. For both sets of observations the transmitter power was lowered to ensure that the echo power did not exceed the maximum sampling level of the digital voltmeters. These measurements were then repeated at a somewhat higher power to establish the dependence in the region 0-2.4 msec and yielded the results plotted in Fig. 1. Finally, observations made with 30 μsec, 100 μsec and 200 μsec pulses and corresponding sample intervals of 20 μsec, 100 μsec and 200 μsec were used to establish the curve in the region 2.4-11.6 msec. These observations are plotted in Fig. 2. Since the antenna beam of the Millstone radar has a half power beam-width comparable to the angular extent of the moon it was necessary to correct the observations for the non-uniform illumination of the moon's surface. The antenna radiation pattern (Fig. 3) was established using radio stars and a distant beacon transmitter as sources. Both methods agreed well and Fig. 3

presents a pattern obtained by averaging plots obtained for the azimuthal and elevation planes. Since the moon has a diameter of 0.5^{o} the antenna corrections required are not large, and amount to only 4 db at the limbs. (Note that the antenna weights the transmission and reception equally so that the effect must be included twice.) In Figs. 1 and 2 we have shown the corrected curve of echo power vs. delay P(t) obtained when the effect of the antenna has been removed. The three corrected curves were next replotted as functions of the logarithm of the echo delay t and overlaid to obtain a single smooth curve. In this way the effect of the saturation of the receiver at the leading edge which was encountered when attempting to observe the limbs could be removed. Figure 4 shows the results obtained. The values plotted in Fig. 4 together with the values observed at 3.6 cm and 68 cm wavelength by Evans and Pettengill (1963b) are listed in Table III. Figure 5 shows the results obtained at the three wavelengths when pulses of 30 μsecs are used to resolve the leading edge. These three curves have been normalized at the origin and are the only results at different wavelengths in which exactly the same resolution was employed. Table III gives the results obtained when shorter (10 μsec) pulses were included in the measurements at 23 and 68 cm.

IVb. Observations of the Depolarized Component

By receiving the same sense of circular polarization as was transmitted it is possible to determine the amount of power that has been converted into the orthogonal circularly polarized mode. Evans and Pettengill (1963b) called this component the "depolarized" component, though additional measurements using linearily polarized waves are required if the complete scattering matrix for the surface is to be established. Measurements of the depolarized and polarized components could be made simultaneously, or alternately at will. Figure 6 shows the distribution of echo power D(t) vs. delay obtained for the depolarized component using 160 μsec pulses, 50 Kc/sec predetection filters and a sample interval of 160 μsec up to a delay of 4 msec and 1 msec pulses, 2 Kc/sec predetection filters and a sample interval of 480 μsec for delays beyond 4 msec. The absolute level of the echo could be established by injecting into the receiver input terminals (via a directional coupler) a pulse of noise corresponding to a known increase in system temperature on each sweep of the timebase. This pulse serves to determine the relationship between

Table III

Relative Echo Power vs. Delay for the Moon

Observed at Lincoln Laboratory M.I.T.

Delay(t)	ϕ°	λ=3.6cm*	23cm†	68cm‡
10 μs.	2.38	0	0	0 db
20 "	3.37	-0.1	-0.85	-0.6 db
30 "	4.11	-0.4	-1.40	-1.5 "
40 "	4.77	-0.55	-1.9	-2.2 "
50 "	5.31	-0.85	-2.35	-2.8 "
60 "	5.83	-1.05	-2.75	-3.3 "
70 "	6.30	-1.35	-3.15	-3.8 "
80 "	6.73	-1.5	-3.55	-4.3 "
90 "	7.13	-1.75	-3.95	-4.8 "
100 "	7.53	-1.95	-4.3	-5.2 "
125 "	8.42	-2.5	-5.05	-6.2 "
150 "	9.22	-2.9	-5.8	-7.0 "
175 "	9.96	-3.4	-6.45	-7.7 "
200 "	10.65	-3.8	-7.0	-8.4 "
225 "	11.30	-4.15	-7.5	-9.0 "
250 "	11.92	-4.45	-8.0	-9.7 "
275 "	12.50	-4.85	-8.45	-10.15"
300 "	13.06	-5.15	-8.85	-10.7 "
325 "	13.60	-5.45	-9.2	-11.1 "
350 "	14.11	-5.75	-9.55	-11.6 "
375 "	14.60	-6.0	-9.9	-11.9 "
400 "	15.09	-6.15	-10.2	-12.35"
425 "	15.56	-6.5	-10.5	-12.7 "
450 "	16.01	-6.70	-10.8	-13.0 "
475 "	16.45	-7.0	-11.2	-13.3 "
500 "	16.88	-7.15	-11.35	-13.6 "
600 "	18.51	-7.9	-12.3	-14.6 "
700 "	20.01	-8.5	-13.2	-15.4 "
800 "	21.40	-9.1	-14.0	-16.2 "
900 "	22.72	-9.55	-14.6	-16.9 "
1000 "	23.96	-9.9	-15.35	-17.6 "
1100 "	25.16	-10.3	-15.95	-18.25"
1200 "	26.29	-10.7	-16.4	-18.9 "
1340 "	27.39	-11.0	-16.8	-19.5 "
1400 "	28.44	-11.3	-17.15	-20.0 "
1500 "	29.42	-11.6	-17.45	-20.4 "

Delay(t)	ϕ°	λ=3.6cm	23cm	68cm
2.0 ms	34.16	-12.9	-18.65	-21.8 d
2.25 "	36.30	-13.5	-19.1	-22.3 "
2.50 "	38.33	-14.0	-19.55	-22.7 "
2.75 "	40.28	-14.35	-19.85	-23.1 "
3.0 "	42.16	-14.85	-20.2	-23.5 "
3.25 "	43.97	-15.1	-20.5	-23.8 "
3.50 "	45.72	-15.4	-20.85	-24.1 "
3.75 "	47.42	-15.7	-21.15	-24.3 "
4.0 "	49.08	-15.9	-21.4	-24.5 "
4.25 "	50.69	-16.1	-21.7	-24.7 "
4.50 "	52.27	-16.35	-21.95	-24.9 "
4.75 "	53.82	-16.5	-22.35	-25.1 "
5.0 "	55.33	-16.7	-22.5	-25.35 "
5.25 "	56.82	-16.9	-22.75	-25.6 "
5.50 "	58.29	-17.1	-23.05	-25.9 "
5.75 "	59.72	-17.35	-23.3	-26.15 "
6.0 "	60.95	-17.6	-23.6	-26.45 "
6.25 "	62.55	-17.85	-23.85	-26.8 "
6.50 "	63.93	-18.1	-24.2	-27.15 "
6.75 "	65.36	-18.35	-24.55	-27.5 "
7.0 "	66.65	-18.6	-24.95	-27.85 "
7.25 "	67.98	-18.9	-25.35	-28.25 "
7.50 "	69.31	-19.2	-25.8	-28.65 "
7.75 "	70.63	-19.45	-26.2	-29.0 "
8.0 "	71.94	-19.75	-26.65	-29.45 "
8.25 "	73.23	-20.1	-27.1	-29.95 "
8.50 "	74.53	-20.4	-27.6	-30.45 "
8.75 "	75.79	-20.8	-28.15	-30.95 "
9.0 "	77.06	-21.2	-28.7	-31.5 "
9.25 "	78.33	-21.6	-29.3	-32.1 "
9.50 "	79.59	-22.1	-29.95	-32.75 "
9.75 "	80.84	-22.6	-30.6	-33.35 "
10.0 "	82.09	-23.1	-31.35	-34.05 "
10.25 "	83.34	|	-32.2	-34.9 "
10.50 "	84.58	|	-33.25	-35.9 "
10.75 "	85.82	Not	-34.35	-36.9 "
11.0 "	87.06	Meas-	-35.85	-38.35 "
11.25 "	88.29	ured	-37.7	-40.1 "
11.50 "	89.53	|	-40.35	-42.7 "

* Pulse = 30 μsec. Resolution at the receiver = 20 μsec.
† Pulse = 10 μsec. Resolution at the receiver = 10 μsec.
‡ Pulse = 12 μsec. Resolution at the receiver = 10 μsec.

D(t) and P(t). In order to remove the effects of pulse length P(t) was redetermined using a 160 μsec pulse and a 50 Kc/s receiver bandwidth. Figure 7 compares the two curves. The percentage polarization p(t) defined in

$$p(t) = \frac{P(t) - D(t)}{P(t) + D(t)} \times 100 \qquad (1)$$

is plotted in Fig. 8. Also shown is the curve for p(t) obtained previously at 68 cm by Evans and Pettengill (1963b). It can be seen that the amount of depolarization has increased with frequency. Two independent sets of measurements are included in Fig. 7. The error bars indicate the uncertainty associated with the points shown as closed circles. The difficulty of establishing the exact relative position of the two curves in Fig. 7 is the major source of uncertainty in measurements of this type. In addition to including a calibration pulse in each measurement it is necessary to establish the waveguide and other losses between the horn feed and the receiver input terminals for the two senses of polarization. This was accomplished using a beacon transmitter coupled to a dipole mounted on a tower in the near field of the antenna. The dipole could be rotated at will without influencing the amount of power radiated by the beacon transmitter. In this way the circularity of the transmission and reception could be checked. The agreement between the two curves in Fig. 7 lends some confidence in the method and suggests that the estimated uncertainty assigned is too large.

IVc. Observations using Linearly Polarized Waves

Additional experiments have been carried out in which linear polarization was transmitted and two orthogonal linear components were received. The transmitted polarization was established using a specially constructed high power polarizer which controlled the energy fed to the antenna feed horns. The degree of linearity achieved could be checked using the remote test dipole and was found to be of the order of 30 db. On reception two orthogonal linear components are obtained, one of which is aligned along the direction of the transmitted polarization. In order to overcome the effects of Faraday rotation in the earth's ionosphere (Browne et al, 1956) the two received signals were recombined in a

second polarizer arrangement consisting of two 3 db combiners and two variable length sections of transmission line (phase shifters). The output of the receiver polarizer was arranged to be a linear component that could be rotated with respect to the transmitted component. The actual angle between the two was established using the test dipole arrangement.

In a preliminary experiment, observations were carried out using 200 μsec pulses. The transmitted plane of polarization was maintained fixed and observations were made for three orientations of the receiver polarization. The observations were carried out in the manner described previously, i.e., a calibration pulse served to establish the absolute echo power. The measurements were made over a short time interval so that the Faraday rotation ($\sim 20^\circ$ two-way at 1295 Mc/s) would not change significantly. The echo power obtained for a given delay interval would be expected to vary sinusoidally through one cycle when the receiver polarization is rotated through an angle of 180°. The peak of the sine wave will correspond to the expected component and the minimum to a component orthogonal to this. The angle between the transmitted plane of polarization and the angle at which the signal is found to peak is simply the two-way Faraday rotation angle. Three points are sufficient to establish the phase and amplitude of a sine wave and hence the measurements obtained for the three received polarizations could be used to determine the ratio of maximum to minimum signal at each delay. This ratio has been plotted in Fig. 9 as a function of delay. It can be seen that in the diffuse region of the echoes (3-11 msec) about 1/8 of the total power is returned in the linear mode orthogonal to that which would be reflected by a plane mirror. The depolarization observed in the circular polarization experiments (Fig. 8) indicates that about 1/3 of the total power is returned in the opposite sense of circular polarization to that expected in this same region. The significance of these ratios are discussed in Sec. V.

IVd. Observations of the Total Radar Cross Section

Previous efforts to obtain reliable total cross section measurements for the moon have been reviewed by Evans and Pettengill (1963c). The errors encountered are usually large, because the uncertainty in the antenna gain

(typically 1 db) enters twice, and uncertainties associated with the determination of the absolute power transmitted and the absolute calibration of the receiver usually are of comparable order.

A very precise determination of the moon's radar cross section is now possible by comparing the lunar echoes with those from a carefully machined metal sphere placed in earth orbit. This sphere, the Lincoln Calibration Sphere (LCS) has a cross section of exactly 1 m^2 at a wavelength of 23 cm (Prosser, 1965). Unfortunately, despite its close range the calibration sphere is a weaker target than the moon by approximately 40 db. Accordingly the full sensitivity of the Millstone Hill radar is required in order to observe it. The procedure adopted in these measurements was as follows. A time was chosen when the moon's elevation and that of the sphere were comparable. The sphere was then tracked using the normal closed-loop tracking afforded by the multiple beam system of the Millstone Hill radar. The automatic tracking system requires the transmission of 2 msec radar pulses. A separate receiver with a bandwidth of 8 Kc/s was used in order to determine the echo amplitude. The output of this receiver was rectified using a square-law detector and sampled at 200 μsec intervals. The integration over the time-base was achieved by summing the digital samples in a computer for consecutive 30 second intervals. Included in the integration process was the normal calibration pulse. About forty successive 30-second integrations were obtained and each of these was used to determine the overall sensitivity of the radar using an appropriate value for the mean range of the satellite during that 30-second period. These observations yielded the following relation:

$$\mathrm{Log}_{10}\, T_{echo} = 18.071 \pm .038 - 4\, \mathrm{Log}_{10}\, R \qquad (2)$$

where T_{echo} is the equivalent increase in the system temperature caused by the satellite echo and R its range. Based upon the parameters of the radar system as determined from independent calibrations (Table II) we should expect

$$\mathrm{Log}_{10}\, T_{echo} = 18.066 - 4\, \mathrm{Log}_{10}\, R \qquad (3)$$

Although in this instance it seems that the radar parameters were in fact quite accurately known prior to this overall calibration, the agreement between (2) and (3) lends considerable confidence to the result reported here.

Following the observations of the LCS sphere the radar was employed to observe the moon in precisely the same way, except that the antenna pointing information was derived from the punched paper tape reader. Since the moon echoes are very much stronger than those from the satellite it was also necessary to reduce the system sensitivity by about 30 db to prevent the receiver from saturating. This was accomplished by reducing the transmitter power by an amount which was measured using a carefully calibrated power meter. It is also possible to achieve the same effect by placing attenuators at the receiver input terminals, but this was considered undesirable as it could disturb the matching of the receiver to the line. The choice of an 8 Kc/s receiver bandwidth was made in order to remove any amplitude fluctuations that might arise from small errors in the automatic compensation of the doppler shift during the observations of the calibration sphere. Observations of moon echoes were made for periods of 30 seconds and a mean of 14 such periods was then taken. Since a 2 msec pulse is less than the full depth of the moon (11.6 msec), at no time was the whole lunar hemisphere illuminated and therefore contributing to the echo power. That is, the cross section $\sigma(T)$ observed with a pulse length of T milliseconds is simply

$$\sigma(T) = \frac{\sigma_o \int_o^T P(t)\, dt}{\int_o^{11.6} P(t)\, dt} \qquad (4)$$

where σ_o is the total cross section. This function is plotted in Fig. 10. When the cross section observed with 2 msec pulses is scaled up to the value for the whole moon we obtain

$$\sigma_o = \pm 0.065 \pm 0.008\ \pi a^2 \qquad (5)$$

The uncertainty given is the rms error resulting from the spread of the values obtained in the 40 observations of the satellite ($\pm$ 0.38 db) and the 14 observations of the moon (also $\pm$ 0.38 db). We believe that the only source of systematic error remaining is that associated with reading the power meter monitoring the transmitter power and the linearity of its scale. These errors are thought to be substantially smaller than the uncertainty quoted.

V. Discussion of the Results

a) The polarized component

The wavelength dependence in the scattering behavior reported initially by Evans and Pettengill (1963b) and supported by Davis and Rohlfs (1964) and Klemperer (1965) is strengthened by these observations. Figure 11 shows all the observations made to date in which a pulse length of 100 μsec or less was employed. That is, Fig. 11 contains the results of all the observations listed in Table I except those of Davis and Rohlfs (1964). The results have been normalized at the origin, but since the resolution achieved in this region varied, it is likely that the absolute relationships between the curves shown in Fig. 11 is slightly in error. In spite of this the wavelength dependence in the results is readily apparent. This behavior must mean that there is a continuum of structure on the lunar surface (or perhaps within the upper layer) having scales in the range of wavelengths that have been employed.

Since there is a direct relation between the echo delay t and the angle of incidence ϕ between the ray and mean surface normal, the angular dependence of the echo power per unit surface area $P(\phi)$ can be examined simply by replotting the echo power as a function of ϕ. In Fig. 12 we have plotted these 23 cm results as a function of log cos ϕ to test whether a law of the form

$$P(\phi) \propto \cos^n \phi \qquad (6)$$

fits the data. The case for the exponent n = 1 would indicate a uniformly bright surface since a pulse of fixed length illuminates a region whose projected area falls as cos ϕ. The case n = 2 would indicate a Lambert law surface. The results shown in Fig. 11 indicate that the region $80^\circ < \phi < 90^\circ$

is uniformly bright (n = 1), but that in the range $50^\circ < \phi < 80^\circ$ the law

$$P(\phi) \propto \cos^{3/2} \phi \qquad (7)$$

is encountered. The behavior shown in Fig. 12 is essentially similar to that reported by Evans and Pettengill (1963b) at 68 cm. No adequate explanation has yet been found for the law (Eq. 7) which lies midway between uniformly bright and Lambert scattering. However, since the surface is nearly uniformly bright we are forced to suppose that the scatterers are nearly isotropic reflectors. Small scale elements having vertical and horizontal dimensions of comparable or smaller size than the wavelength would behave in this fashion. Evans and Pettengill (1963b) argued on this basis that the regions obeying the linear relations plotted in Fig. 12 are those in which the small scale elements of the surface scatter more strongly than the smoother portions – probably because few large elements of the surface are inclined at such large angles to the mean surface. This region (i.e., $\phi \geq 40^\circ$) was termed "diffuse". For $\phi < 40^\circ$ the scattering appears very sensitive to the angle of incidence and hence is attributed to the smoother undulating portions of the surface which can be treated as flat facets. This scattering has been called quasi-specular.

The division of the echo power into two regimes attributable to two broad classes of surface structure has been encountered at all the radio wavelengths employed thus far. Figure 13 shows the results given in Fig. 11 when replotted as a function of 1 + Log cos ϕ. We find that at all wavelengths the region beyond t = 4 msec ($\phi \sim 50^\circ$) the echo power describes a straight line. For wavelengths of 600, 68 and 23 cm the exponent n (Eq. 6) is found to be n = 3/2 and for 3.6 and 0.86 cm it appears to be unity, though here the results are somewhat less certain.

We note that though some authors (e.g., Daniels, 1963 a,b, Rea et al, 1964) have accepted the interpretation of the curves (e.g., Fig. 11) in terms of two classes of scatterer, others (e.g., Muhleman, 1964, Beckmann, 1965) have not, and instead have attempted to explain the complete curve $P(\phi)$ in terms of quasi-specular scattering. This requires that there be substantial amounts of

surface area tilted at very large angles to the mean surface and the rms slope one derives as a result is correspondingly large. We do not think that this view is correct and have argued against it previously (Evans and Hagfors, 1964). Further evidence in support of the model outlined above is available from the work of Katz (1965) who has considered the wavelength dependence of the absolute echo power at given delays. Katz finds that at the leading edge the cross section per unit area increases with wavelength according to a law lying between λ and λ^2. This dependence suggests coherent reflection from facets whose average size increases with increasing wavelength. On the other hand, in the diffuse tail the absolute echo power varies nearly as λ^{-2} implying a totally different scattering mechanism. A similar conslusion has been reached by Peake and Taylor (1963) who compared the results reported by Evans and Pettengill (1963b) with scattering from different types of terrestrial surface. We shall return to this point when discussing the polarization results.

The amount of power associated with the diffuse component of the echoes is listed in Table IV.

Table IV

Percent of the Total Power in the Diffuse Component

λ = 68 cm	20%
λ = 23 cm	25%
λ = 3.6 cm	35%
λ = 0.86 cm	85%

When the diffuse component of the power, i.e., that corresponding to the straight-lines in Fig. 13 has been subtracted, the remainder observed at 3.6, 23 and 68 cm appears as plotted in Fig. 14. This component of the power is related to the distribution of surface slopes and will be discussed further under Sec. VI. We have been unable to find any simple empirical law to describe this component, which, by adjusting a single constant, will match the results at all wavelengths.

Evans and Pettengill proposed a law of the form $P(\phi) \propto (1 + b\,\phi^2)^{-1}$, but a more careful computation of the power in the quasi-specular component (presented in Fig. 14) shows that this law is inexact. Good agreement can be obtained with a law published by Hagfors (1964) that has been derived from theoretical considerations (Sec. VI).

b. The Depolarization Results

The measurements reported in Sections IV b and c are open to two possible types of explanation, namely a) some elements of the surface may have small radii of curvature and as such can act as dipoles, and b) the reflection coefficient may depend upon the relation between the plane of polarization and the local plane of incidence. Thus, for example, multiple reflections may occur, one of which is near the Brewster angle, or the echo may be partly reflected from within the lunar surface and hence depend upon the transmission coefficient into the uppermost layer.

Evans and Pettengill (1963b) attributed the depolarization to effect a). Hagfors et al (1965) have shown, however, that for $\phi > 40^\circ$ it appears that the echo is entirely reflected from within the lunar surface and as such the echo power from any small region depends upon the square of the local transmission coefficient. Since the transmission coefficients for waves polarized in and normal to the local plane of incidence are different and any one range ring includes all possible local planes of incidence, this will serve to cause some depolarization. However, it appears that the magnitude of an effect of this type is inadequate to account for the large amount of depolarization observed in Fig. 7. Stated otherwise, although an effect of type b) is demonstrably present in lunar reflection the original explanation a) proposed by Evans and Pettengill (1963b) appears correct. We note that Long (1965) invokes a similar explanation in attempting to account for the polarization of radar echoes from the sea at grazing incidence.

The echoes from the quasi-specular region are little depolarized and this is to be expected for reflections from a largely smooth undulating surface (Hagfors, 1964). There is, however, a marked transition at about 3 msec delay (Figs. 8 and 9) beyond which the amount of depolarization is roughly constant.

We may model the scatterers in this region as flat facets which do not depolarize and a random collection of dipoles which do. Randomly arranged dipoles would completely depolarize an incident circularly polarized wave, since they would destroy the $\lambda/4$ phase relationship between the two linears into which a circular wave may be resolved. Thus in order to account for amount of polarization (about 40%) observed at t = 8 msec (Fig. 8) we require that roughly 40% of the energy be returned from the facets and 60% from the dipoles. In this case the dipoles will split their reflections equally between the two components to give 30% in the depolarized component and 70% will appear in the expected sense — as is observed. When linearly polarized waves are employed the dipoles reflect in the incident and orthogonal planes in the ratio 3:1 (Mack and Reiffen, 1964). It follows that of the 60% of the power reflected by the dipoles only 1/4, i.e., 15%, will be in the sense orthogonal to the transmitted mode. Thus the ratio between the two components would be expected to be about 0.18, i.e., in fair agreement with the results shown in Fig. 9.

Some support for the model proposed here is given in Fig. 15 where we have plotted the echo power observed in the opposite sense circular mode to the expected sense [i.e., D(t) shown in Fig. 6] as a function of Log (cos ϕ). We find that the echo power conforms to the law $D(\phi) \propto \cos \phi$, which is similar to the law observed for the diffuse component of the expected signal. A law $D(\phi) \propto \cos \phi$ was also observed at 68 cm (Evans and Pettengill, 1963b).

It should be understood that this modeling of the surface as a collection of facets and dipoles is merely a convenient fiction which serves to describe the electrical performance of the surface. We do not suppose that the lunar surface is covered with dipoles, but merely that there are elements having small radii of curvature and as such force the induced currents to flow in preferred directions different from that of the field exciting them. Thus we see that the results of the circular and linearly polarized experiments are both open to a common explanation. Furthermore, these results support the view advanced earlier that the scattering in the diffuse region is dissimilar from that of the center of the disk. Attempts to describe the entire scattering law on the basis of quasi-specular scattering (e.g., Beckmann, 1965) may

succeed in matching the observed curves, but this should not be construed as an indication of the physical reality of the model.

c. The Radar Cross Section σ_o

Many observers have reported values of σ_o and some of these are presented in Table V and plotted in Fig. 16. The values have been presented as fractions of the physical cross section of the moon ($\pi a^2 = 9.49 \times 10^{12}$ m^2) and span a range of over ten octaves (from 8.6 mm to 22 meters). The increase in cross section with increasing wavelength suggested by Fig. 16 depends largely on the three long wave measurements reported by Davis and Rohlfs (1964). These measurements may have been subject to systematic errors introduced by ionospheric effects. If these three points are ignored the remainder show no clear wavelength dependence. In part this is caused by the large error bars associated with each measurement which may conceal a marked dependence. The errors given in Table V are the reported values where these have been given, or $\pm$ 3 db where no uncertainty was published.

The errors associated with these measurements are generally large for reasons we have already enumerated. It seems that a reliable determination of the cross section vs wavelength would require that each radar be calibrated in the manner described in Sec. IV d.

The scattering cross section expected for a large dielectric sphere may be written (Evans and Pettengill, 1963b)

$$\sigma_o = g \rho_o \pi a^2 \qquad (8)$$

where ρ_o is the Fresnel reflection coefficient for normal incidence and g a term which denotes the directivity of the target, i.e., the ability to scatter preferentially toward the radar. In the case of a perfect sphere g = 1 and for the case where the surface has large scale irregularities (but is locally smooth on the scale of at least a wavelength) $g = 1 + \alpha^2$, where α^2 is the mean square

Table V

Values for the Radar Cross Section of the Moon as a Function of Wavelength Reported by Various Workers

Author	Year	Wavelength(cm)	$\sigma/\pi a^2$	Estimated Error db
Lynn et al	1963	0.86	0.07	± 1.
Kobrin	1963*	3.0	0.07	± 1.
Morrow et al	1963*	3.6	0.07	± 1.5
Evans and Pettengill	1963c	3.6	0.04	± 3.
Kobrin	1963*	10.0	0.07	± 1.
Hughes	1963*	10.0	0.05	± 3.
Victor et al	1961	12.5	0.022	± 3.
This paper	1965	23	0.065	± 0.5
Aarons	1959**	33.5	0.09	± 3.
Blevis and Chapman	1960	61.0	0.05	± 3.
Fricker et al	1960	73.0	0.074	± 1.
Leadabrand	1959**	75.0	0.10	± 3.
Trexler	1958	100.0	0.07	± 4.
Aarons	1959**	149.0	0.07	± 3.
Trexler	1958	150.0	0.08	± 4.
Webb	1959**	199.0	0.05	± 3.
Evans	1957	250.0	0.10	± 3.
Evans et al	1959	300.0	0.10	± 3.
Evans and Ingalls	1962	784.0	0.06	± 5.
Davis and Rohlfs	1964	1130.0	0.19	+ 3. - 2.
Davis and Rohlfs	1964	1560.0	0.13	+ 3. - 2.
Davis and Rohlfs	1964	1920.0	0.16	+ 3

---

* Revised value – (privately communicated to Evans and Pettengill, 1963c).

**Reported by Senior and Siegel (1959, 1960).

surface slope (Hagfors, 1964). For the general case in which the sphere is covered with structure having scales down to and smaller than the wavelength in size, g has not been evaluated quantitatively. If the surface is completely covered in structure comparable with the wavelength and as a result behaves as a Lambert scatterer, then g = 8/3 (Grieg et al, 1948). It is thought, therefore, that as the surface is covered to an increasing extent with objects comparable in size to the wavelength, g increases from unity toward a value of about 3 or possibly higher.

For the long wave measurements ($\lambda \geq 1$ m) shown in Fig. 15 we conclude that $g \approx 1.0$ but that g increases for $\lambda < 1$ m. The absence of a corresponding increase in σ_o indicates that ρ_o is decreasing with wavelength, and hence suggests that the reflection arises in an inhomogeneous surface. If the density of the material on the lunar surface increases with depth then the longest waves will penetrate deepest and the effective reflection coefficient will increase accordingly.

From the 68 cm results Evans and Pettengill (1963b) derived a reflection coefficient $\rho_o = 0.064$ after attempting to subtract out the echo power attributable to the diffuse component. By assuming that the electrical conductivity of the lunar surface is zero and hence the dielectric constant $k = (1 + \sqrt{\rho_o})^2/(1 - \sqrt{\rho_o})^2$ Evans and Pettengill derived a value $k = 2.8$. Rea et al (1964) used the same experimental results, but employed a somewhat more rigorous method of removing the echo power attributable to the rough structure (for which the value of g is not known) and obtained $k = 2.6$. These radar values, although very low when compared with the values observed for terrestrial rocks (Brunschwig et al, 1960) are in fact considerably higher than values obtained in passive radiometric observations. Perhaps the most reliable method of deriving k in such studies is to determine the degree of polarization exhibited by the radio emission, since this depends directly upon the transmission coefficient of the surface $(1 - \rho_o)$ and thus on the dielectric constant k (Troitsky, 1954). Measurements of this kind have been performed by a number of observers (e.g., Soboleva, 1962; Heiles and Drake, 1963; Mezger, 1965; Davies and Gardner, 1965) and yield values chiefly in the range $k = 1.7$ to $k = 2.1$. Other values obtained by studying the thermal history of the moon over a lunation are less direct but also yield

values in the range 1.5 to 2.0 (e.g., Troitsky, 1962; Salomonovich and Losovsky, 1962; Krotikov and Troitsky, 1962). The discrepancy between the radar and passive results has long remained a puzzle. Calculations by one of us (Hagfors and Morriello, 1965) of the effect of surface roughness on the interpretation of the passive observations has indicated that, though this does tend to lower the value of k that is derived, the effect is not large enough to account for the discrepancy. The difficulty seems resolved as a result of recent radar observations reported by Hagfors et al (1965) which indicate that the radar echoes at normal incidence are partially reflected from within the lunar surface, and that the upper layer has a dielectric constant of only about 1.8. It seems therefore that the passive measurements refer to the uppermost material (extending in depth perhaps some tens of centimeters) and that the radar reflections yield an average value related somehow to the way in which the density increases as a function of depth.

Giraud (1965) has examined the way in which the reflection coefficient would vary in the case of a surface in which the density increases from zero linearly with depth over a distance of d to a density corresponding to a dielectric constant k_1. On the basis of this model only when $\lambda > 20$ d is the reflection coefficient the same as that which would be attributed to the subsurface layer in the absence of an inhomogeneous covering. If the measurements listed in Table V could be repeated with an accuracy equal to that reported in this paper it seems that the depth of the layer of light material overlying the lunar surface might be established.

VI. Scattering from an undulating surface

The results reported by Evans and Pettengill (1963b) have stimulated a large number of investigators to attempt a physical description of the lunar surface from the observations. Broadly two types of theories have been advanced. In one, ray optics are employed and the surface considered to be an assemblage of flat facets, each of which reflects back to the radar only if viewed at normal incidence. This treatment avoids the difficulty encountered in other approaches in that the reflection coefficient is simply the Fresnel reflection coefficient at normal incidence ρ_o and does not depend on the angle of incidence. Brown (1960), Muhleman (1964) and Rea et al (1964) have

developed theories employing this approach which differ in the way in which the statistical description of the sizes and shapes of the facets are handled. Rea et al (1964) derive a relation between the angular power spectrum and the probability density $f(\phi)$. Here $f(\phi).d\omega$ is the probability that the surface normal lies within the solid angle element $d\omega$ which makes an angle ϕ with the normal to the mean surface. They find that the angular power spectrum is given by:

$$\bar{P}(\phi)\, d\phi \propto \frac{f(\phi)\, d\phi\, dS}{\cos \phi} \tag{9}$$

This model can be expected to apply only to the quasi-specular portions of the echo (Fig. 14) where the scattering arises chiefly from regions having large radii of curvature. The mean surface slope averaged over all possible vertical planes is given in

$$\bar{\phi} = \frac{\int_\phi \phi\, f(\phi) \sin \phi\, d\phi}{\int_\phi f(\phi) \sin \phi\, d\phi} = \frac{\int_\phi \phi\, \bar{P}(\phi) \cos \phi \sin \phi\, d\phi}{\int_\phi \bar{P}(\phi) \cos \phi \sin \phi\, d\phi} \tag{10}$$

Values of $\bar{\phi}$ have been obtained by numerically integrating Eq. 10 and employing for $\bar{P}(\phi)$ the curves shown in Fig. 14. The values obtained are at $\lambda = 68$ cm, $\bar{\phi} = 10.2^\circ$ and at 3.6 cm $\bar{\phi} = 14.8^\circ$. In order to obtain these results it was necessary to extrapolate the results for $P(\phi)$ for the region $\phi < 3^\circ$. This was accomplished as shown in Fig. 17, by fitting a linear law to the values of Log $P(\phi)$ observed in the range $4^\circ < \phi < 10^\circ$. The uncertainty associated with this procedure introduces an uncertainty of perhaps $\pm 1^\circ$ in the values given for $\bar{\phi}$.

In a second approach diffraction theory is employed. The surface is treated as locally smooth (so that the boundary conditions can be established using Fresnel's reflection formula) and undulating. The probability of finding a point on the surface at a height h above the mean surface is generally assumed to be gaussian, i.e., proportional to $\exp\left[-\frac{1}{2}(h/h_o)^2\right]$ where h_o is the rms height fluctuation. The horizontal behavior of the surface is then

specified by means of an autocorrelation function $\rho(d)$ where

$$\rho(d) = \frac{\overline{h(x)\, h(x+d)}}{(h_o)^2} \tag{11}$$

in which $h(x)$ is the height of the surface at a point x and $h(x+d)$ at a distance d away. Both exponential [$\rho(d) \propto \exp\,(-d/d')$] and gaussian [$\rho(d) \propto \exp\,(-\frac{1}{2}(d/d_o)^2)$] functions have been examined. Most workers have avoided the difficulty encountered due to the reflection coefficient varying with the angle of incidence ϕ by assuming the surface to be perfectly conducting (e.g., Hargreaves 1959; Daniels 1961; Hagfors 1961; Hayre and Moore 1961; Bramley 1962; Hughes 1962 a, b,; Winter 1962; Fung and Moore 1964). Hagfors (1964) has treated the case of a dielectric sphere and shown that when allowance is made for the curvature of the moon's surface and the physically most plausible series of approximations for the terms in the expression for the reflected field (Huygen's integral) are made, the following results are obtained.

Gaussian $$\rho(d) \propto \exp\left[-\frac{1}{2}\left(\frac{d}{d_o}^2\right)\right] \tag{12}$$

$$P(\phi) \propto \frac{\exp\,[-\phi^2/2\,\phi_o^{\,2}]}{\cos^4\phi} \tag{13}$$

where $\phi_o = h_o/d_o$

Exponential $$\rho(d) \propto \exp\left(-\frac{d}{d'}\right) \tag{14}$$

$$P(\phi) \propto \left\{\frac{1}{\cos^4\phi + C\sin^2\phi}\right\}^{3/2} \tag{15}$$

where $C = [d'\,\lambda/4\,\pi\,h_o^{\,2}]^2$

Hagfors (1965) has shown that if the statistics of the surface slopes are made the same in the geometric optics and in the autocorrelation approaches the two methods will yield the same results provided the surface introduces deep phase modulation and provided only large scale structure is present on the surface. Physically this may be taken as a demonstration that the regions oriented normal to the line of sight are mainly effective in scattering back to the radar.

The experimental results presented in Fig. 14 have been compared with the laws Eq. 13 and Eq. 15 and in each case it has been found that the exponential surface best matches the results. In this case, it should be noted a direct comparison of the geometric optics and the autocorrelation approaches is very difficult due to the presence of an appreciable amount of small scale structure.

Table VI lists values of the relative echo power (expressed in db) as a function of the angle of incidence ϕ according to Eq. 15 for various values of the parameter C. The values of C which match the experimental results are at λ = 68 cm C = 100, λ = 23 cm C = 70, λ = 3.6 cm C = 30. It should be noted that these are the values that match the quasi-specular component of the echoes (i.e., after the diffuse component has been subtracted). Slightly lower values would be required if one attempted to match the whole curve for $P(\phi)$. It is evident that the constant C does not vary as λ^2 as expected (Eq. 15). Furthermore, if the known rms height of the lunar mountains ($\sim$ 1 Km) is inserted for h_o one obtains a value for the correlation distance d' larger than the size of the moon. This has led Daniels (1961) to suggest that the term h_o in Eq. 15 should not be associated with the largest elements on the lunar surface. Fung and Moore (1964) have advanced similar arguments. Beckmann (1965) has attempted to allow formally for a wavelength dependence in the value C (other than $C \propto \lambda^2$) by considering the surface as a sum of many components (e.g., mountains, hills, hummocks, craters,...) each of which has heights that are gaussianly distributed and is describable by means of an exponential autocorrelation function. The scattering law (Beckmann, 1965) obtained is identical to that given by Hagfors (1964) in Eq. 15 except that the constant C becomes $C = [\sum_{i=1}^{i_{max}} d_i' \lambda^2/4\pi \Sigma h_o'_i]^2$ where i is an integer indicating the ith component of the surface. Since at normal incidence structure for which $h_o < \lambda/8$ introduces little perturbation in the reflected phase front and may be neglected, a wavelength dependent i_{max} may be determined and the wavelength dependence follows.

TABLE VI

Reduction in Relative Echo Power (db) vs Angle of Incidence ϕ according to Eq. 15

ANGLE ϕ	C = 10	25	32	50	70	95	100
0	.0	.0	.0	.0	.0	.0	.0
1	.0	.0	.0	.0	.1	.2	.2
2	.0	.2	.2	.4	.5	.7	.7
3	.1	.4	.5	.8	1.1	1.5	1.5
4	.2	.7	.9	1.4	1.9	2.4	2.5
5	.4	1.0	1.3	2.0	2.7	3.5	3.6
6	.5	1.5	1.8	2.7	3.6	4.6	4.7
7	.7	1.9	2.4	3.5	4.5	5.7	5.9
8	.9	2.4	3.0	4.3	5.5	6.7	6.9
9	1.2	2.9	3.6	5.1	6.4	7.7	8.0
10	1.4	3.4	4.2	5.8	7.3	8.7	9.0
11	1.7	4.0	4.8	6.6	8.1	9.6	9.9
12	1.9	4.5	5.4	7.3	8.9	10.5	10.8
13	2.2	5.0	6.0	8.0	9.7	11.3	11.6
14	2.5	5.6	6.6	8.7	10.5	12.1	12.4
15	2.8	6.1	7.2	9.4	11.2	12.9	13.2
16	3.1	6.6	7.7	10.0	11.9	13.6	13.9
17	3.4	7.1	8.3	10.6	12.5	14.3	14.6
18	3.7	7.6	8.8	11.2	13.1	14.9	15.2
19	4.0	8.1	9.3	11.8	13.7	15.5	15.9
20	4.3	8.5	9.8	12.3	14.3	16.1	16.4
21	4.7	9.0	10.3	12.8	14.8	16.7	17.0
22	5.0	9.4	10.8	13.3	15.4	17.2	17.5
23	5.3	9.8	11.2	13.8	15.9	17.7	18.1
24	5.6	10.3	11.7	14.3	16.3	18.2	18.5
25	5.9	10.7	12.1	14.7	16.8	18.7	19.0
26	6.2	11.1	12.5	15.2	17.2	19.1	19.5
27	6.4	11.4	12.9	15.6	17.7	19.6	19.9
28	6.7	11.8	13.3	16.0	18.1	20.0	20.3
29	7.0	12.2	13.6	16.4	18.5	20.4	20.7
30	7.3	12.5	14.0	16.7	18.9	20.8	21.1
31	7.6	12.8	14.3	17.1	19.2	21.2	21.5
32	7.8	13.2	14.7	17.4	19.6	21.5	21.8
33	8.1	13.5	15.0	17.8	19.9	21.9	22.2
34	8.3	13.8	15.3	18.1	20.2	22.2	22.5
35	8.6	14.1	15.6	18.4	20.6	22.5	22.8
36	8.8	14.4	15.9	18.7	20.9	22.8	23.2
37	9.1	14.6	16.2	19.0	21.2	23.1	23.5
38	9.3	14.9	16.5	19.3	21.5	23.4	23.7
39	9.5	15.2	16.7	19.6	21.7	23.7	24.0
40	9.8	15.4	17.0	19.8	22.0	24.0	24.3
41	10.0	15.7	17.2	20.1	22.3	24.2	24.6
42	10.2	15.9	17.5	20.3	22.5	24.5	24.8
43	10.4	16.1	17.7	20.6	22.7	24.7	25.1
44	10.6	16.4	17.9	20.8	23.0	25.0	25.3
45	10.8	16.6	18.2	21.0	23.2	25.2	25.5
46	11.0	16.8	18.4	21.3	23.4	25.4	25.7
47	11.2	17.0	18.6	21.5	23.6	25.6	26.0
48	11.4	17.2	18.8	21.7	23.8	25.8	26.2
49	11.5	17.4	19.0	21.9	24.0	26.0	26.4

It should be stressed that the theory outlined here, like the ray optics treatment, can be expected to apply only to the quasi-specular component of the echoes. The diffuse component of the echoes we have associated with the small scale elements of the surface for reasons advanced in Sec. V a,b. Some authors (e.g., Muhleman, 1964; Beckmann, 1965; Beckmann and Klemperer, 1965) have, however, attempted to explain the whole curve for $P(\phi)$ using one of the theories outlined here, and in some instances have been surprisingly successful in matching the observed curves by one of a family predicted by the theory. Unfortunately, as we remarked earlier however, this cannot be taken as proof of the validity of the physical premises upon which the theory is based.

In the diffuse region it appears that diffraction of the waves around small objects will be an important effect. Hagfors et al (1965) have shown that the scattering in this region is likely to take place entirely within the lunar surface and hence the small objects may lie upon a subsurface layer or may be density irregularities in the uppermost layer.

Beckmann (1965) has developed a theory which includes the geometric effects of shadowing and this theory has been applied to the lunar results by Beckmann and Klemperer (1965). Apart from the objection we have raised to treating the diffuse echoes as attributable to quasi-specular scattering we believe that the shadowing function derived by Beckmann (1965) is in error. This function specifies the amount of surface area that will be removed from view at grazing angles. There appears to be a mathematical mistake in the derivation of this function (Shaw, 1966), but we do not believe that this is the proper function to employ in any event. A little thought serves to show that the elements of the surface which are capable of reflecting back to the radar are the very ones which introduce most of the shadowing. Since the regions that are shadowed are the reverse slopes of the mountains (which would not reflect favorably) it is largely the regions which would not contribute to the reflection that are screened from view. It follows that the shadowing effect is less severe than would be supposed by assuming a dependence simply on the amount of area removed from view. By modeling a surface in a digital computer the above statement has been verified, and this work is the subject of a separate paper (Brockelman and Hagfors, 1966).

VII. Conclusion

Experiments have been reported in which the scattering behavior of the moon at a wavelength of 23 cm has been investigated. The wavelength dependence observed by earlier workers has been supported by these measurements. By employing different polarizations for transmission and reception the depolarizing properties have been explored. These results support the view that the scattering from the center of the disk is largely from regions that are locally smooth on the scale of the wavelength, whereas for an angle of incidence $\phi > 40^{\circ}$ scattering from rough structure appears to predominate. In the central region the theory of the scattering is in satisfactory shape, and the surface can be described as having an exponential autocorrelation function and a mean slope of about 10° when measured over an interval of a few meters. In the limb region where scattering from rough structure predominates the theory is less satisfactory. The scatterers may be modeled as collections of dipoles and flat facets, and at 23 cm wavelength 60% of the power is reflected by the dipoles. This irregular structure, must, however, largely lie within the surface according to separate experiments reported by Hagfors et al (1965). The depth and perhaps some other properties of the uppermost tenuous layer might be inferred if very precise radar cross section measurements could be made at many wavelengths. The paper outlines one method of accomplishing this using a precisely machined calibration sphere in Earth orbit as a radar reference standard.

Acknowledgments

We are indebted to many of our colleagues for assistance with the experiments described herein. Mr. J. Morriello was responsible for writing the computer program which provided us with an ephemeris, and R. A. Brockelman for the computer program required in the data averaging. Mr. V. C. Pineo has provided considerable advice and constant encouragement. The successful operation of the equipment depended upon a number of individuals that includes H. J. Camacho, H. H. Danforth, E. N. Dupont, G. M. Hyde, L. B. Hanson, L. G. Kraft, R. C. Smith and O. S. Thompson. The use of the facilities of the Lincoln Laboratory Millstone/Haystack complex, provided by the U. S. Air Force, is gratefully acknowledged.

sk

Figure Legends

Fig. 1 Observations of moon echoes over the range of delays t = 0 to t = 2.4 msec. These observations were performed using pulses of 10 and 30 μsec length.

Fig. 2 Observations of moon echoes over the full range of delays 0 – 11.6 msec. using pulses of 30, 100 and 200 μsec. The curve shown "broken" has been obtained by correcting the observations for the effect of the non-uniform illumination introduced by the antenna beam.

Fig. 3 The antenna pattern for the Millstone Hill radar obtained by scanning radio stars and a distant beacon transmitter. The antenna pattern shown here imposes a weighting of the results both on transmission and reception. The effect of this weighting is indicated in Figs. 1 and 2.

Fig. 4 The combined results of all the measurements are included in this plot to obtain the complete dependence of echo power with delay.

Fig. 5 The 23 cm results shown in Fig. 2 are here compared with results reported by Evans and Pettengill (1963b) at 3.6 and 68 cm wavelength. For all three curves the shortest pulse measurements that have been included was 30 μsec, so that the resolution near zero delay is comparable. All the curves have been normalized at the origin.

Fig. 6 The depolarized or opposite sense circularly polarized mode observed at 23 cm wavelength. This curve was obtained using a 160 μsec pulse to explore the region up to 4 msec delay and a 1 msec pulse for the region beyond.

Fig. 7 The results shown in Fig. 6 are here compared to scale with a determination of the expected component of the echo power. These results were obtained using a 160 μsec transmitter pulse on February 3, 1966.

Fig. 8 The percentage polarization (defined in the text) observed for the circularly polarized components (Fig. 7) is plotted here together with previous results for 68 cm (Evans and Pettengill, 1963b). It appears that there is a larger amount of depolarization at 23 cm than at 68 cm.

Fig. 9 The effect of the moon's reflection properties on linearly polarized signals is plotted in this diagram. It can be seen that little energy is converted from the incident linear mode into an orthogonal mode for small values of delay (corresponding to near normal incidence). There appears a break at 3 msec delay (see also Fig. 8) and this is attributed to the transition from largely quasi-specular to largely diffuse reflection.

Fig. 10 The variation of the total cross section of the moon at 23 cm wavelength as a function of pulse length. This curve was derived from the results presented in Fig. 4 and has been employed in obtaining an accurate determination of the radar cross section of the moon (See IVd).

Fig. 11 This plot summarizes the radar observations of the moon reported thus far in which a pulse length of 100 μsec or shorter was employed. All the curves have been normalized at zero delay. Although the resolution of the echo near t = 0 differed considerably between the experiments (and hence the relative positions of the curves is likely to be somewhat in error) the wavelength dependence in the scattering is clearly evident.

Fig. 12 The results obtained for the expected component of the echoes (Fig. 2) have been replotted as a function of Log cos ϕ. We find that in the region $\phi \geq 80^\circ$ the echo power is proportional to cos ϕ and for $50^\circ < \phi < 80^\circ$ to cos $^{3/2}$ ϕ. Similar behavior was observed at 68 cm wavelength (Evans and Pettengill, 1963b), but the reason for this dependence is not clearly understood.

Fig. 13 The results plotted in Fig. 11 are here replotted as a function of Log cos ϕ. We find that the region beyond 4 msec delay (termed diffuse in the text) conforms to a simple dependence upon either cos ϕ (λ = 0.8 cm and 3.6 cm) or cos $^{3/2}$ ϕ (λ = 23, 68, and 600 cm).

Fig. 14 The quasi-specular component of the echoes, i.e., the echo power remaining when the component following the straight lines in Fig. 13 has been subtracted. There seems little difference between the results at λ = 23 and λ = 68 cm, indicating that at these two wavelengths the distribution of surface slopes appears to be about the same.

Fig. 15 The angular scattering law for the depolarized component of the echoes D(t) plotted in Fig. 6.

Fig. 16 The cross section of the moon vs. wavelength.

Fig. 17 The behavior of the echo power for small values of ϕ. Because of the finite length of the pulses the behavior in the region $\phi < 2.5^{\circ}$ has not been explored it has been necessary to extrapolate the results linearly as shown in order to obtain values for the mean surface slope $\overline{\phi}$ (see text).

REFERENCES

Beckmann, P., "Radar backscattering from the surface of the moon", J. Geophys. Res., 70, 2345-2350 (1965).

Beckmann, P., and W. K. Klemperer, "Interpretation of the angular dependence of backscattering from the moon and Venus", J. Res. NBS, 69D, 12 (1965).

Blevis, B. C., and J. H. Chapman, "Characteristics of 488 megacycles per second radio signals reflected from the moon", J. Res. NBS, 64D, 331-334 (1960).

Bramley, E.N., "A note on the theory of moon echoes", Proc. Phys. Soc., 80, 1128-1132 (1962).

Brockelman, R. A., and T. Hagfors, "Note on the effect of shadowing on the backscattering of waves from a random rough surface", to be published (1966).

Brown, E. W., "A lunar and planetary echo theory", J. Geophys. Res., 65, 3087-3095 (1960).

Browne, I. C., J. V. Evans, J. K. Hargreaves, and W. A. S. Murray, "Radio echoes from the moon", Proc. Phys. Soc., B69, 901-920 (1956).

Brunschwig, M., et al (10 authors), "Estimation of the physical constants of the lunar surface", The University of Michigan Rep. 3544-1-F, (1960).

Daniels, F. B., "A theory of radar reflection from the moon and planets", J. Geophys. Res., 66, 1781-1788 (1961).

Daniels, F. B., "Radar determination of the root mean square slope of the lunar surface", J. Geophys. Res., 68, 449-453 (1963a).

Daniels, F. B., "Radar determination of lunar slopes: Correction for the diffuse component", J. Geophys. Res., 68, 2864-2865 (1963b).

Davies, R. D., and F. F. Gardner, "Linear Polarization of Lunar Emission," J. Res. NBS, 69D, 1613, (1965).

Davis, J. R., and D. C. Rohlfs, "Lunar radio-reflection properties at decameter wavelengths," J. Geophys. Res., 69, 3257-3262, (1964).

Evans, J. V., "The Scattering of Radiowaves by the Moon," Proc. Phys. Soc., B70, 1105-1112, (1957).

Evans, J. V., "Radar studies of the moon," J. Res. NBS, 69D, 1637-1659, (1965).

Evans, J. V., R. A. Brockelman, J. C. Henry, G. M. Hyde, L. G. Kraft, W. A. Reid and W. W. Smith, "Radio echo observations of Venus and Mercury at 23 cm wavelength", Astron. J., 70, 486-501, (1965).

Evans, J. V., S. Evans, and J. H. Thomson, "The rapid fading of moon echoes at 100 Mc/s", Paris Symposium on Radio Astronomy, (ed. R. N. Bracewell), p. 8, Stanford University Press, Stanford (1959).

Evans, J. V., and T. Hagfors, "On the interpretation of radar reflections from the moon", Icarus, 3, 151-160 (1964).

Evans, J. V., and R. P. Ingalls, "Radio echo studies of the moon at 7.84-meter wavelength", MIT Lincoln Lab. Tech. Rep. 288, ASTIA No. DDC204008 (1962).

Evans, J. V., and G. H. Pettengill, "The scattering properties of the lunar surface at radio wavelengths", in The Moon, Meteorites and Comets – The Solar System, Vol. 4 (ed. G. P. Kuiper and B. M. Middlehurst), Chapter 5, Univ. of Chicago Press, Chicago (1963a).

Evans, J. V., and G. H. Pettengill, "The scattering behavior of the moon at wavelengths of 3.6, 68, and 784 centimeters", J. Geophys. Res., 68, 423-447 (1963b).

Evans, J. V., and G. H. Pettengill, "The radar cross-section of the moon", J. Geophys. Res., 68, 5098-5099 (1963c).

Fricker, S. J., R. P. Ingalls, W. C. Mason, M. L. Stone, and D. W. Swift, "Computation and measurement of the fading rate of moon-reflected UHF signals", J. Res. NBS, 64D, 455-465 (1960).

Fung, A. K., and R. K. Moore, "Effects of structure size on moon and earth radar returns at various angles", J. Geophys. Res., 69, 1075-1081 (1964).

Giraud, A., "Note on the radio reflectivity of the lunar surface," J. Res. NBS, 69D, 1677-1681, (1965).

Grieg, D. D., S. Metzger, and R. Waer, "Considerations of moon-relay communication", Proc. IRE, 36, 652-663 (1948).

Hagfors, T., "Some properties of radio waves reflected from the moon and their relation to the lunar surface", J. Geophys. Res., 66, 777-785 (1961).

Hagfors, T., "Backscattering from an undulating surface with applications to radar returns from the moon", J. Geophys. Res., 69, 3779-3784 (1964).

Hagfors, T., "The Relationship of Geometric Optics and Autocorrelation Approaches to the Analysis of Lunar and Planetary Radar", J. Geophys. Res., 71, 379-383 (1966).

Hagfors, T., and J. E. Morriello, "The effect of roughness on the polarization of thermal emission from a surface", J. Res. NBS, 69D, 1614-1615 (1965).

Hagfors, T., R. A. Brockelman, H. H. Danforth, L. B. Hanson and G. M. Hyde, "Tenuous surface layer on the moon. Evidence derived from radar observations", Science, 150, 1153-1156 (1965).

Hargreaves, J. K., "Radio observations of the lunar surface", Proc. Phys. Soc. B73, 536-537 (1959).

Hayre, H. S., and R. K. Moore, "Theoretical scattering coefficient for near vertical incidence from contour maps", J. Res. NBS, 65D, 427-432 (1961).

Heacock, R. L., G. P. Kuiper, E. M. Shoemaker, H. C. Urey and E. A. Whitaker, "Ranger VII, Part II Experimenters' Analyses and Interpretations", Jet Propulsion Laboratory T.R. 32-700 (1965).

Heiles, C. E., and F. D. Drake, "The polarization and intensity of thermal radiation from a planetary surface" Icarus, 2, 281-292 (1963).

Hughes, V. A., "Radio wave scattering from the lunar surface", Proc. Phys. Soc., 78, 988-997 (1961).

Hughes, V. A., "Diffraction theory applied to radio wave scattering from the lunar surface", Proc. Phys. Soc., 80, 1117-1127 (1962a).

Hughes, V. A., "Discussion of paper by Daniels 'A theory of radar reflections from the moon and planets", J. Geophys. Res., 67, 892-894 (1962b).

Katz, I., "The microwave colour of the earth and the moon," paper presented to the IEEE International Meeting on Antennas and Propagation, Washington, D. C., September (1965).

Klemperer, W. K., "Angular scattering law for the moon at 6-meter wavelength," J. Geophys. Res., 70, 3798-3800, (1965).

Krotikov, V. D., and Troitsky, V. S., "The emissivity of the moon at centimeter wavelengths," A. J. USSR, 39, 1089-1093, (1962).

Long, M. W., "On the polarization and wavelength dependence of sea echo," IEEE Trans. Antennas and Propagation, AP 13, 749-754, (1965).

Lynn, V. L., M. D. Sohigian, and E. A. Crocker, "Radar observations of the moon at 8.6 mm wavelength," MIT Lincoln Lab. Tech. Rep. 331, ASTIA No. DDC 426207, (1963). See also, J. Geophys. Res., 69, 781-783, (1964).

Markov, A. V., "Brightness distribution over the lunar disk at full moon," Astron. J. USSR 25, 172-179, (1948).

Mack, C. L., and B. Reiffen, "RF characteristics of thin dipoles," Proc. IEEE 52, 533-542, (1964).

Mezger, P. G., "Polarization of thermal radiation of the moon at 14.5 Gc/s," J. Res. NBS 69D, 1612 (1965).

Muhleman, D. O., "Radar scattering from Venus and the Moon," Astron. J., 69, 34-41 (1964).

Peake, W. H., and R. C. Taylor, "Radar backscattering measurements from 'moon-like' surfaces," Ohio State University E.E. Dept. Report 1388-9, (1963).

Pettengill, G. H., and J. C. Henry, "Radio measurements of the lunar surface," in The Moon, IAU Symposium 14, (ed. Z. Kopal and Z. K. Mikhailov), p. 519, Academic Press, London (1962).

Prosser, R. T., "The Lincoln Calibration Sphere," Proc. IEEE, 53, 1672, (1965).

Rea, D. G., N. Hetherington, and R. Mifflin, "The analysis of radar echoes from the moon," J. Geophys. Res., 69, 5217-5223, (1964).

Salomonovich, A. E., and B. Y. Losovsky, "Radio brightness distribution of the lunar disk at 0.8 cm," Astron. J. USSR, 39, 1074-1082, (1962).

Senior, T. B. A., and K. M. Siegel, "Radar reflection characteristics of the moon", in Paris Symposium on Radio Astronomy (ed. R. N. Bracewell) p. 29 Stanford University Press, Stanford, (1959).

Senior, T. B. A., and K. M. Siegel, "A theory of radar scattering by the moon", J. Res. NBS, 64D, 217-228 (1960).

Shaw, L., "Comments on shadowing of random surfaces", submitted to IEEE Trans. AP (1965).

Soboleva, N. S., "Measurement of the polarization of lunar radio emission on a wavelength of 3.2 cm", Astron. J. USSR, 39, 1124-1126 (1962).

Trexler, J. H., "Lunar radio echoes", Proc. IRE, 46, 286-292 (1958).

Troitsky, V. S., "Theory of lunar radio emission", Astron. J. USSR, 31, 511-528 (1954).

Troitsky, V. S., "Radio emission of the moon, its physical state and the nature of its surface", in The Moon, IAU Symposium 14, (ed. Z. Kopal and Z. K. Mikhailov), p. 475, Academic Press, London (1962).

Victor, W. K., R. Stevens, and S. W. Golomb, "Radar exploration of Venus", Jet Propulsion Lab. Tech. Rep. 32-132 (1961).

Winter, D. V., "A theory of radar reflections from a rough moon", J. Res. NBS, 66D, 215-226 (1962).

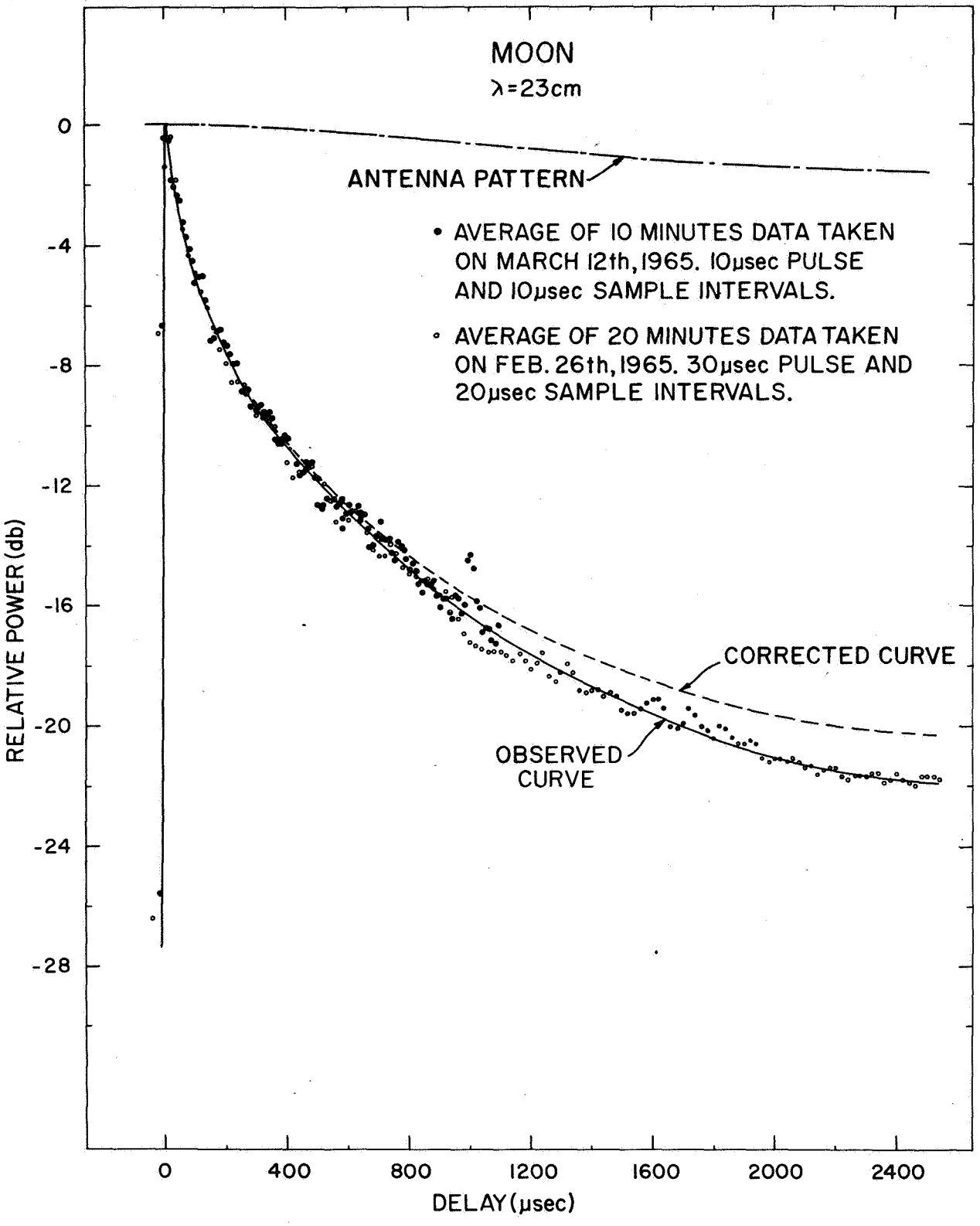
MOON
λ=23cm
ANTENNA PATTERN
• AVERAGE OF 10 MINUTES DATA TAKEN ON MARCH 12th, 1965. 10μsec PULSE AND 10μsec SAMPLE INTERVALS.
◦ AVERAGE OF 20 MINUTES DATA TAKEN ON FEB. 26th, 1965. 30μsec PULSE AND 20μsec SAMPLE INTERVALS.
CORRECTED CURVE
OBSERVED CURVE
RELATIVE POWER (db)
0
-4
-8
-12
-16
-20
-24
-28
0
400
800
1200
1600
2000
2400
DELAY (μsec)

Fig. 1

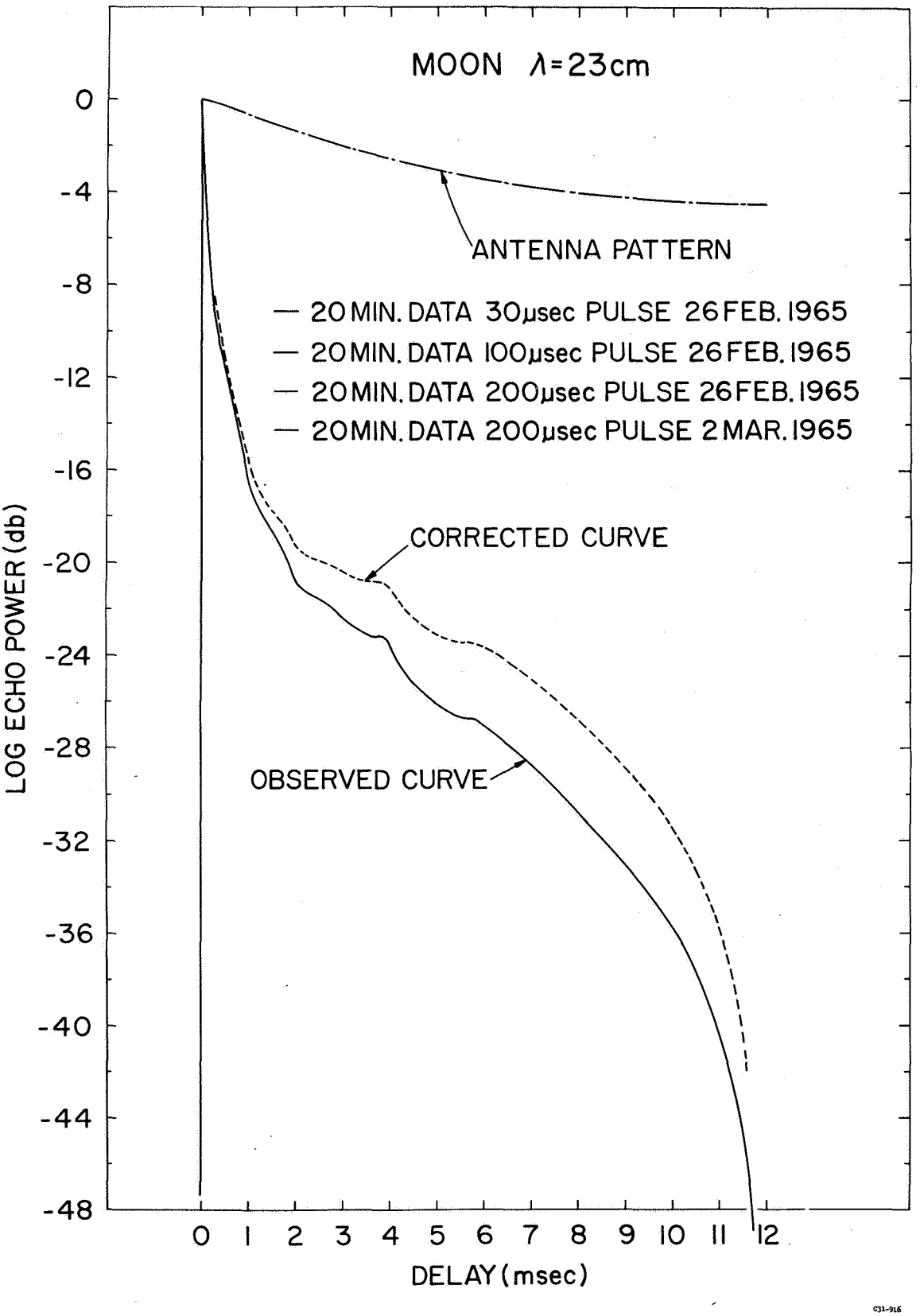
MOON λ=23cm
ANTENNA PATTERN
— 20 MIN. DATA 30μsec PULSE 26 FEB. 1965
— 20 MIN. DATA 100μsec PULSE 26 FEB. 1965
— 20 MIN. DATA 200μsec PULSE 26 FEB. 1965
— 20 MIN. DATA 200μsec PULSE 2 MAR. 1965
CORRECTED CURVE
OBSERVED CURVE
LOG ECHO POWER (db)
0
-4
-8
-12
-16
-20
-24
-28
-32
-36
-40
-44
-48
0 1 2 3 4 5 6 7 8 9 10 11 12
DELAY (msec)
C31-916

Fig. 2

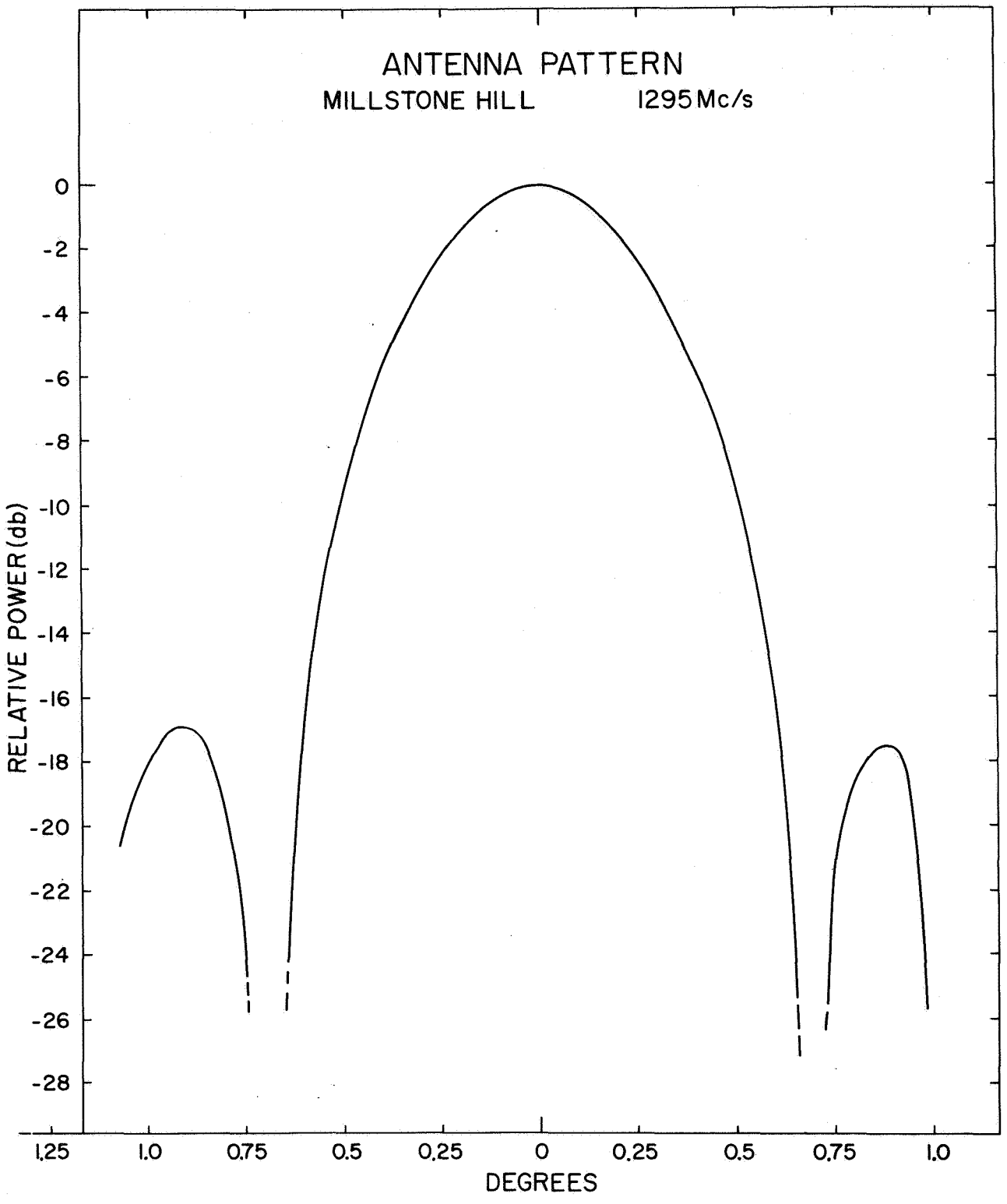
ANTENNA PATTERN
MILLSTONE HILL
1295 Mc/s
RELATIVE POWER (db)
0
-2
-4
-6
-8
-10
-12
-14
-16
-18
-20
-22
-24
-26
-28
1.25
1.0
0.75
0.5
0.25
0
0.25
0.5
0.75
1.0
DEGREES

Fig. 3

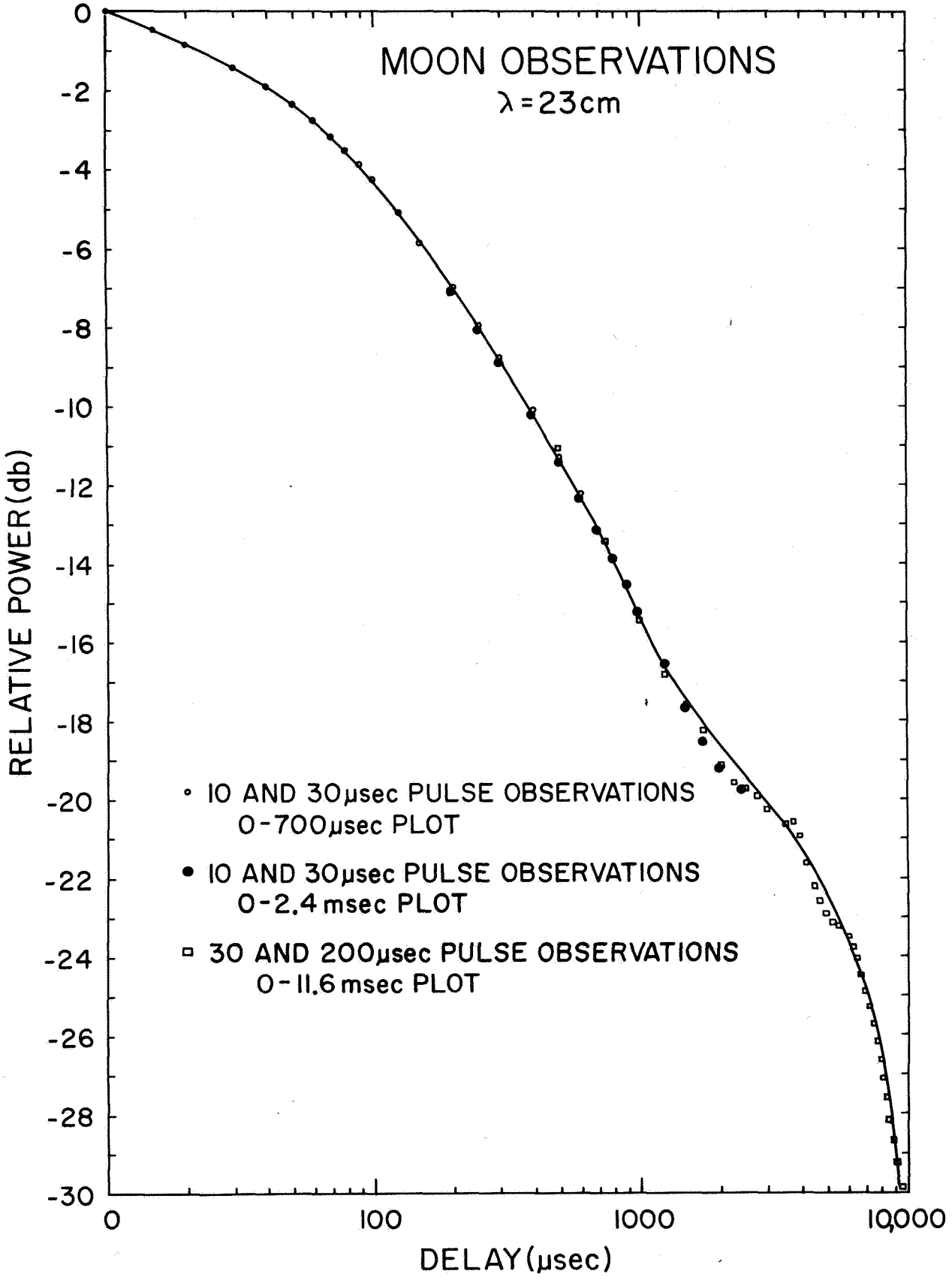
MOON OBSERVATIONS
λ = 23cm
RELATIVE POWER (db)
0
-2
-4
-6
-8
-10
-12
-14
-16
-18
-20
-22
-24
-26
-28
-30
0
100
1000
10,000
DELAY (μsec)
° 10 AND 30 μsec PULSE OBSERVATIONS
0-700 μsec PLOT
• 10 AND 30 μsec PULSE OBSERVATIONS
0-2.4 msec PLOT
□ 30 AND 200 μsec PULSE OBSERVATIONS
0-11.6 msec PLOT

Fig. 4

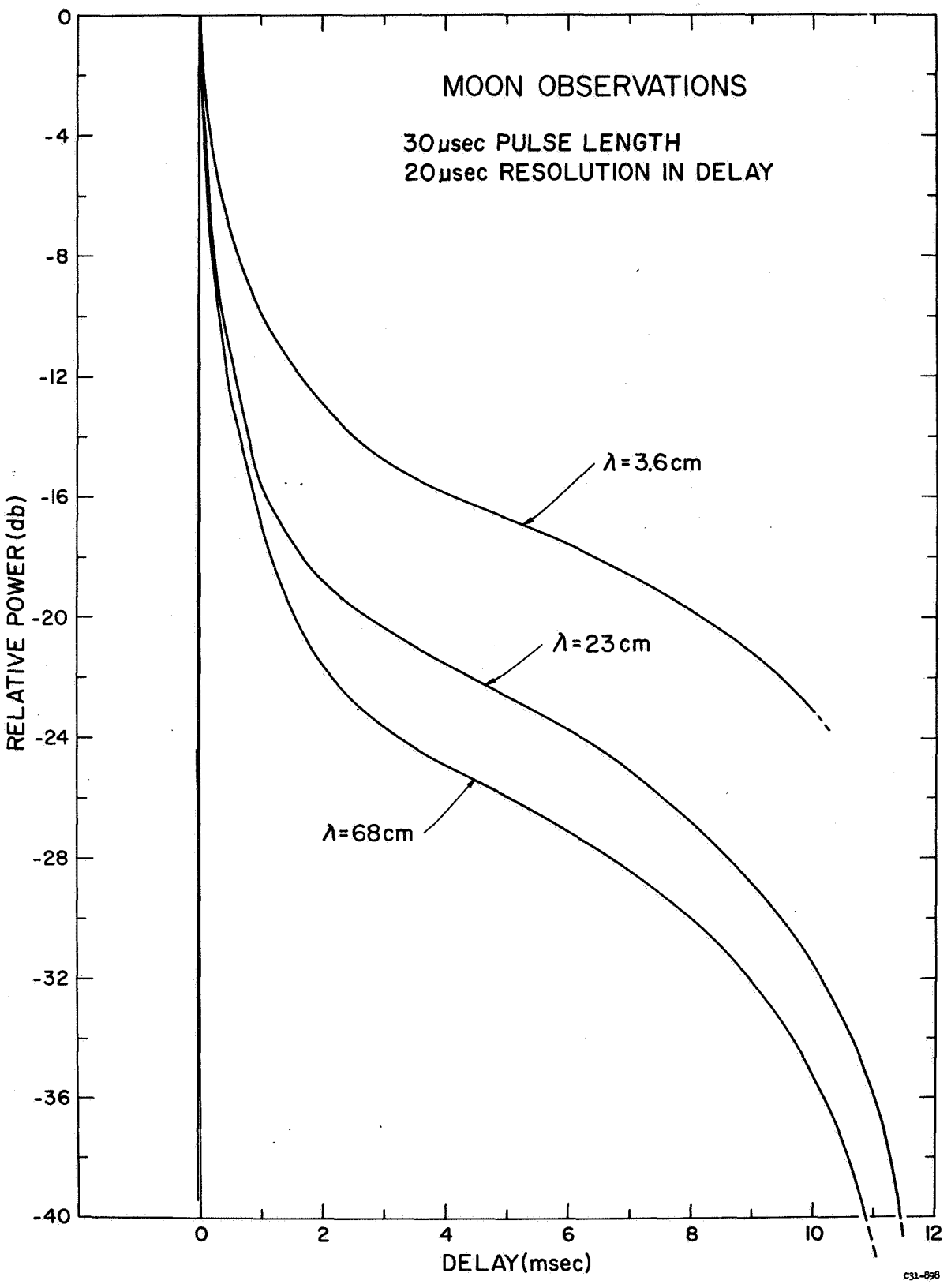
MOON OBSERVATIONS
30 μsec PULSE LENGTH
20 μsec RESOLUTION IN DELAY
λ = 3.6 cm
λ = 23 cm
λ = 68 cm
RELATIVE POWER (db)
0
-4
-8
-12
-16
-20
-24
-28
-32
-36
-40
0
2
4
6
8
10
12
DELAY (msec)
C31-898

Fig. 5

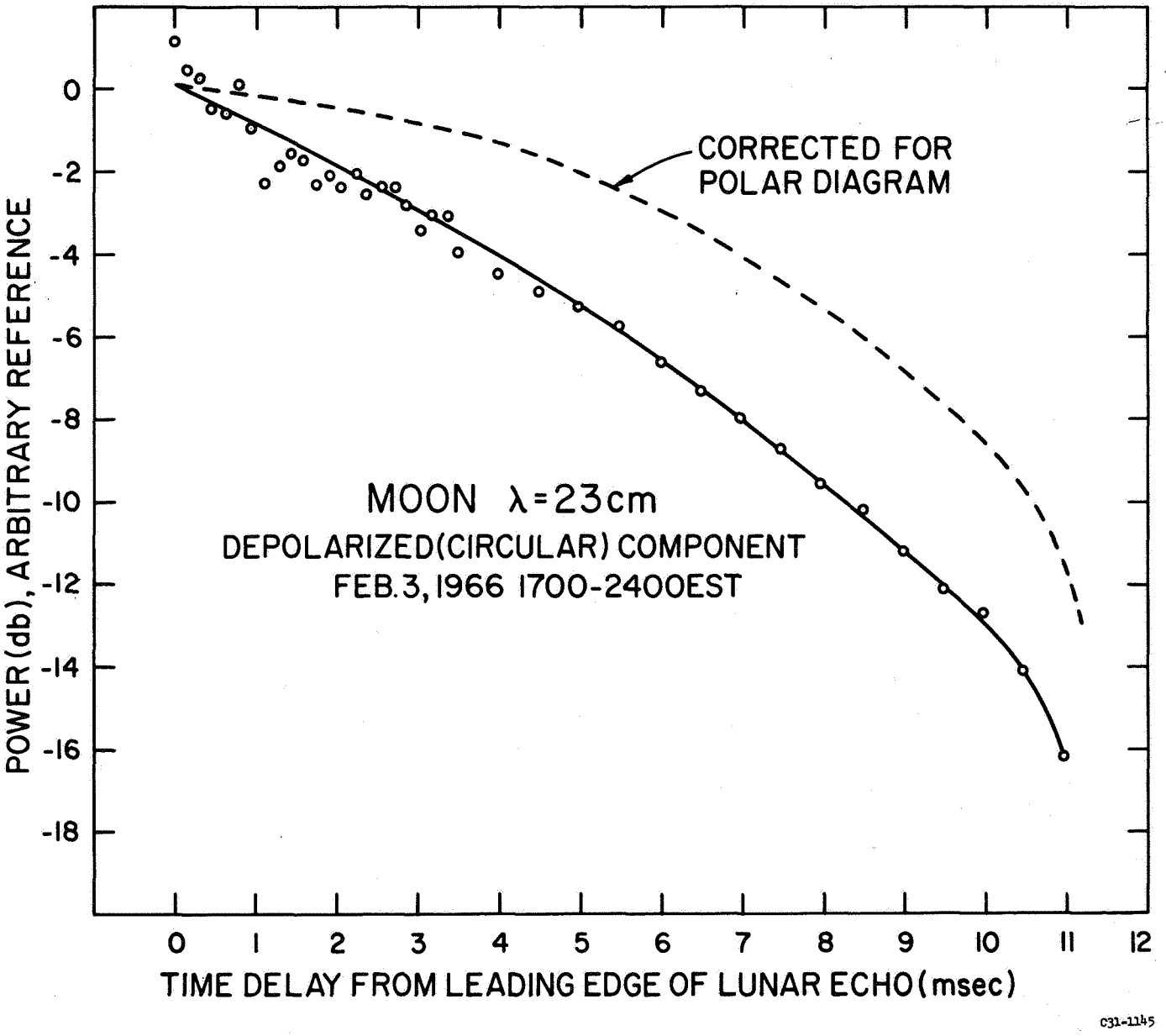
POWER (db), ARBITRARY REFERENCE
0
-2
-4
-6
-8
-10
-12
-14
-16
-18
CORRECTED FOR
POLAR DIAGRAM
MOON λ=23cm
DEPOLARIZED(CIRCULAR) COMPONENT
FEB. 3, 1966 1700-2400EST
0 1 2 3 4 5 6 7 8 9 10 11 12
TIME DELAY FROM LEADING EDGE OF LUNAR ECHO (msec)
C31-1145

Fig. 6

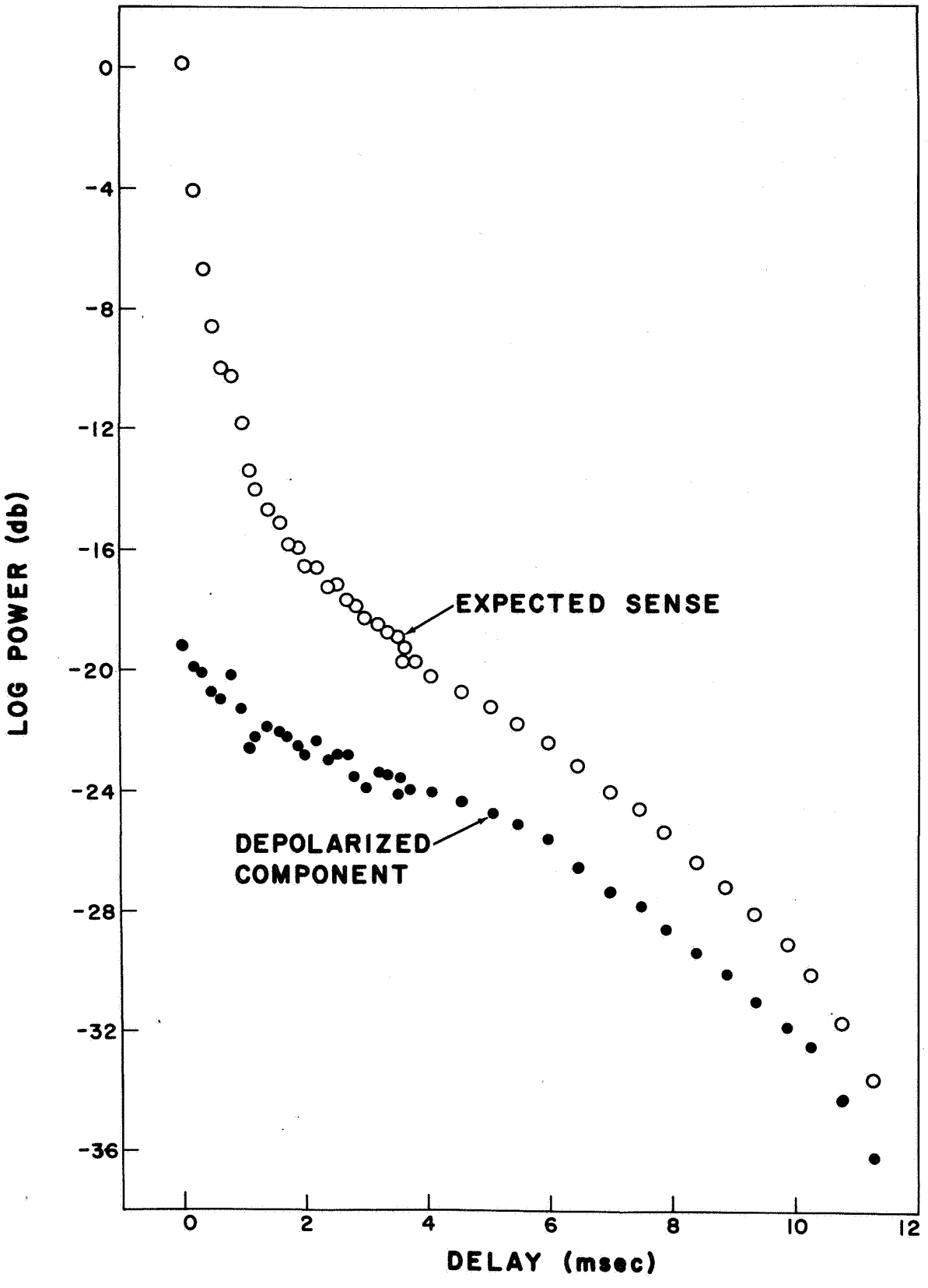
LOG POWER (db)
0
-4
-8
-12
-16
-20
-24
-28
-32
-36
EXPECTED SENSE
DEPOLARIZED
COMPONENT
0
2
4
6
8
10
12
DELAY (msec)

Fig. 7

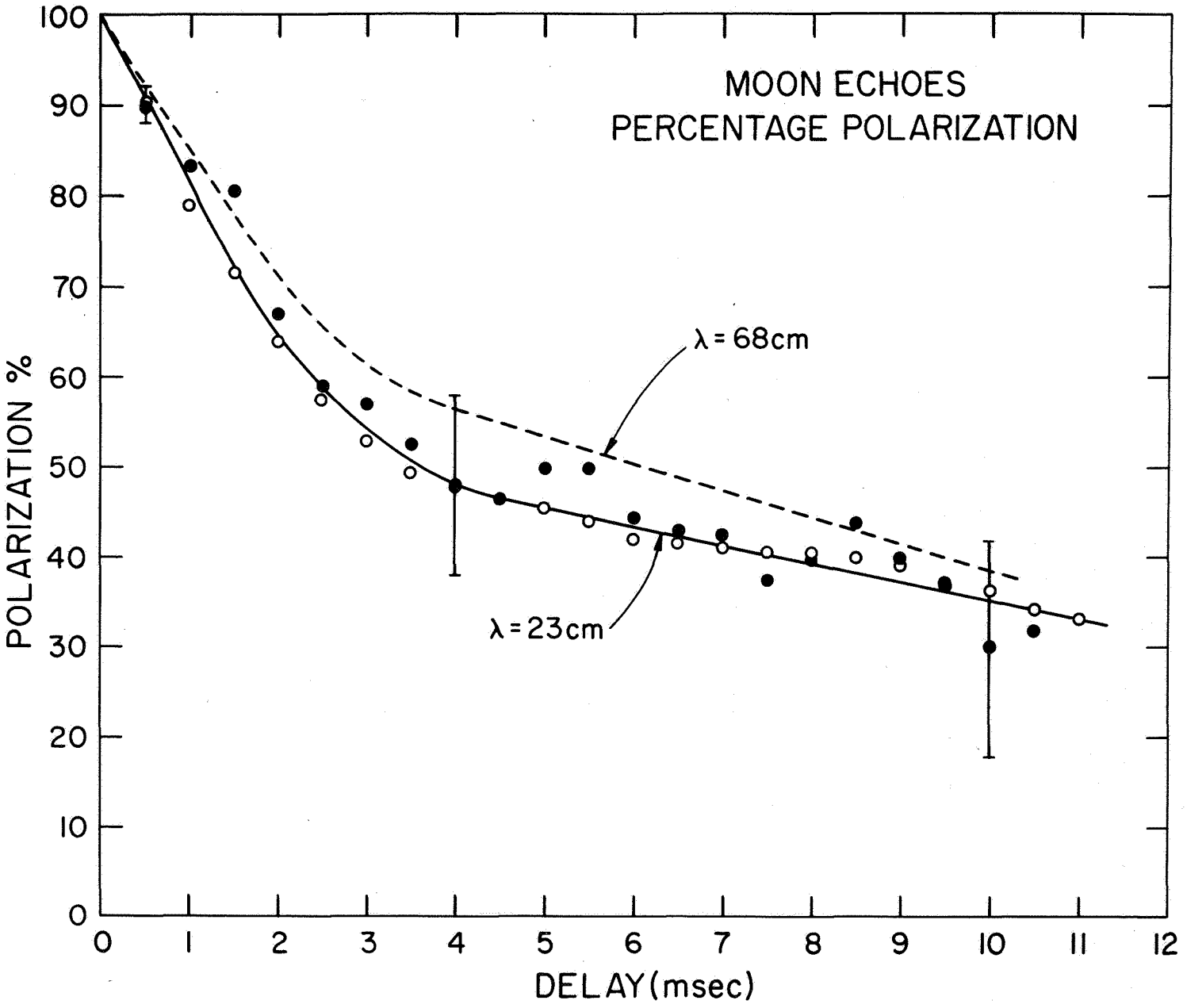
MOON ECHOES
PERCENTAGE POLARIZATION
λ = 68cm
λ = 23cm
POLARIZATION %
DELAY (msec)
100
90
80
70
60
50
40
30
20
10
0
0
1
2
3
4
5
6
7
8
9
10
11
12

Fig. 8

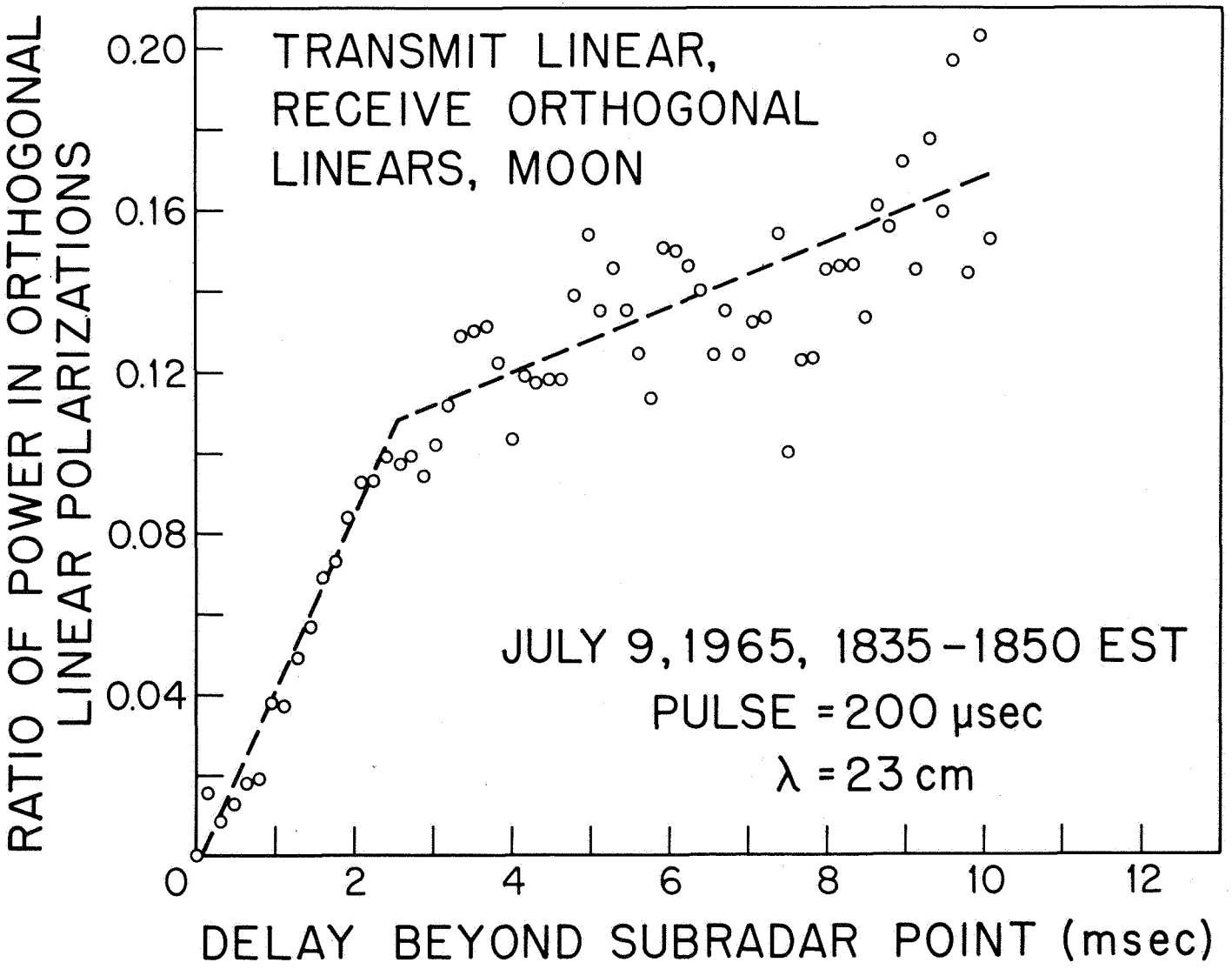
TRANSMIT LINEAR,
RECEIVE ORTHOGONAL
LINEARS, MOON
JULY 9, 1965, 1835-1850 EST
PULSE = 200 μsec
λ = 23 cm
RATIO OF POWER IN ORTHOGONAL LINEAR POLARIZATIONS
0.20
0.16
0.12
0.08
0.04
0
2
4
6
8
10
12
DELAY BEYOND SUBRADAR POINT (msec)

Fig. 9

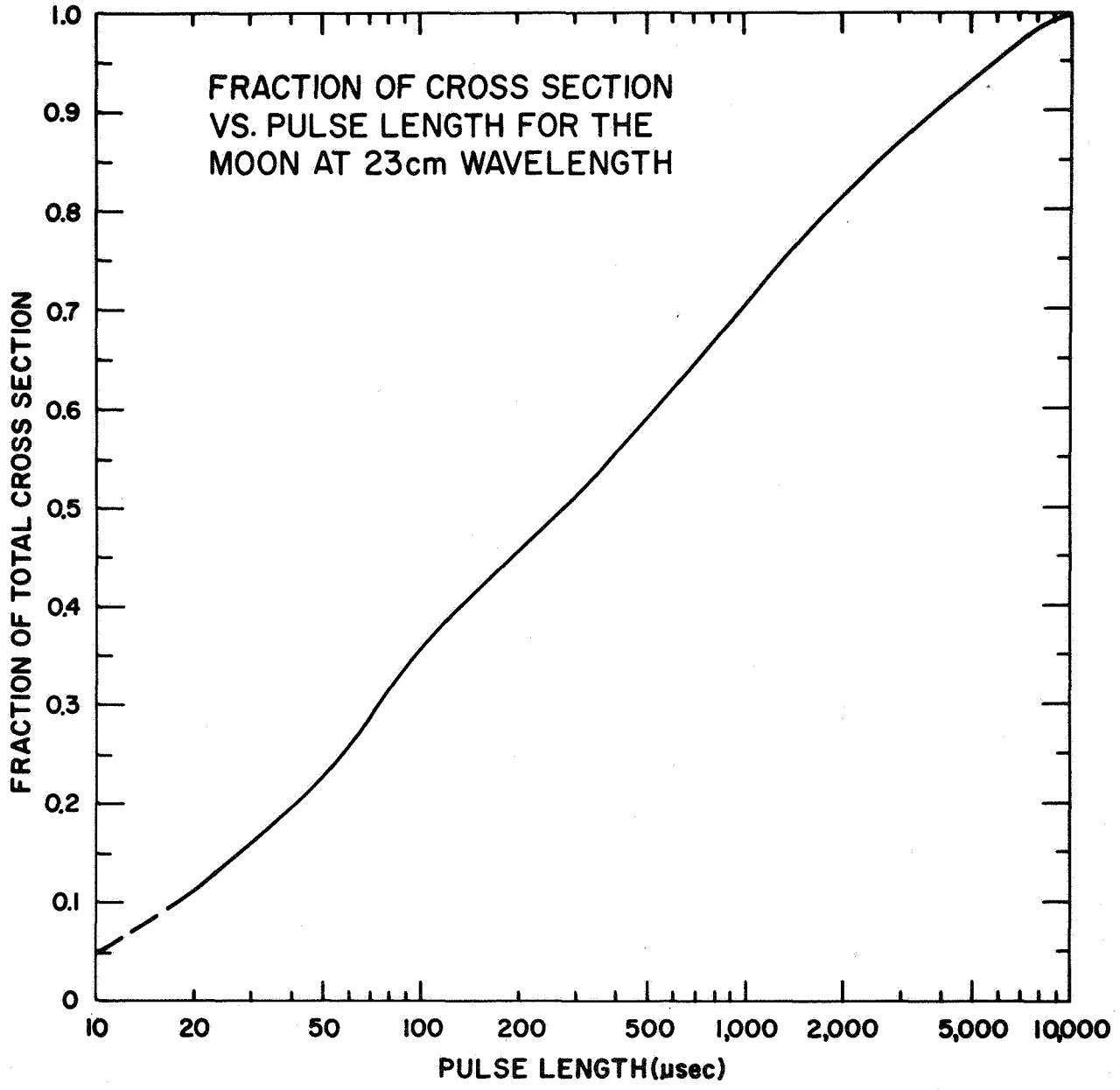

C31-1045

Fig. 10

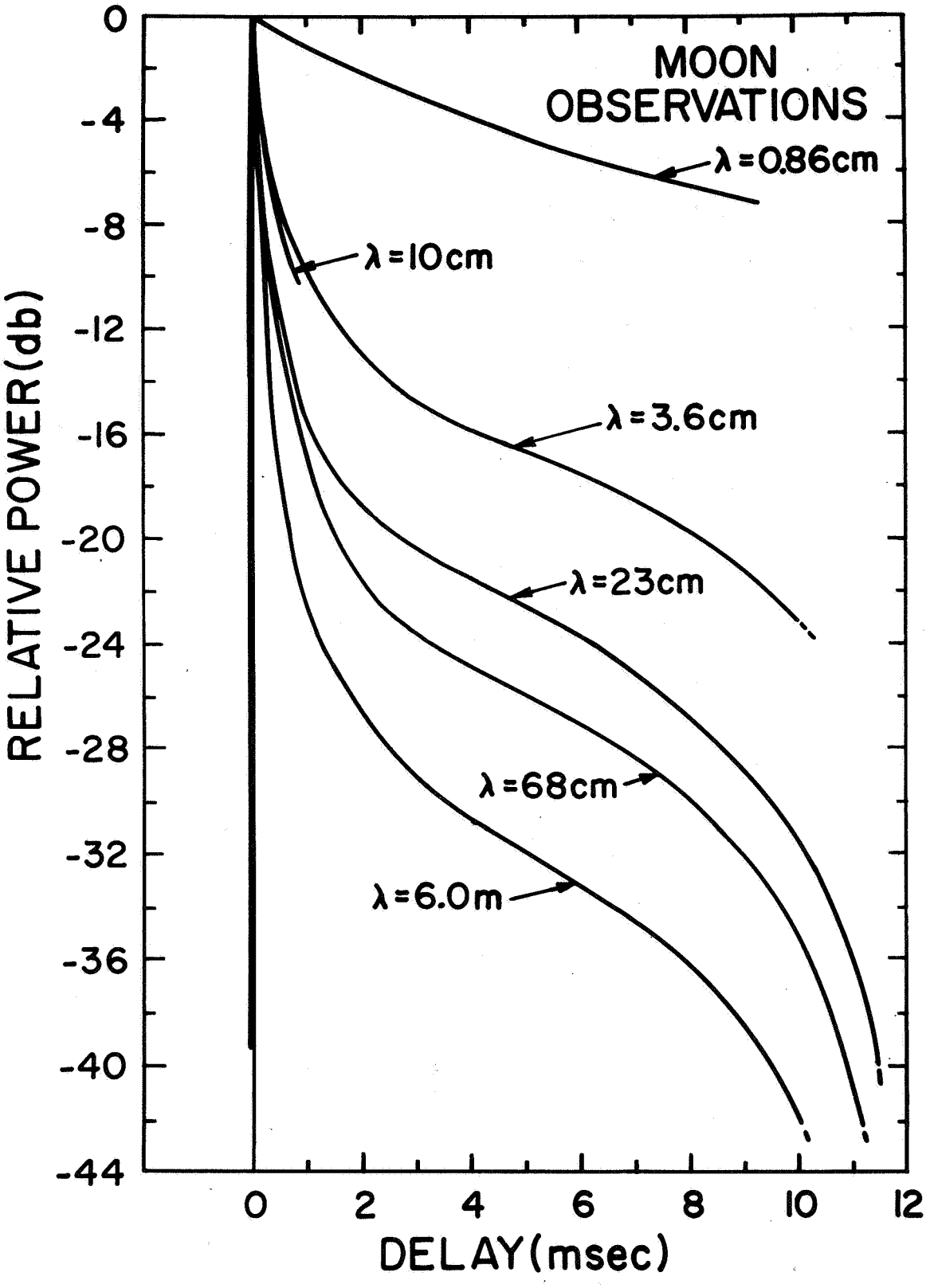
MOON
OBSERVATIONS
λ=0.86cm
λ=10cm
λ=3.6cm
λ=23cm
λ=68cm
λ=6.0m
RELATIVE POWER(db)
0
-4
-8
-12
-16
-20
-24
-28
-32
-36
-40
-44
0
2
4
6
8
10
12
DELAY(msec)

Fig. 11

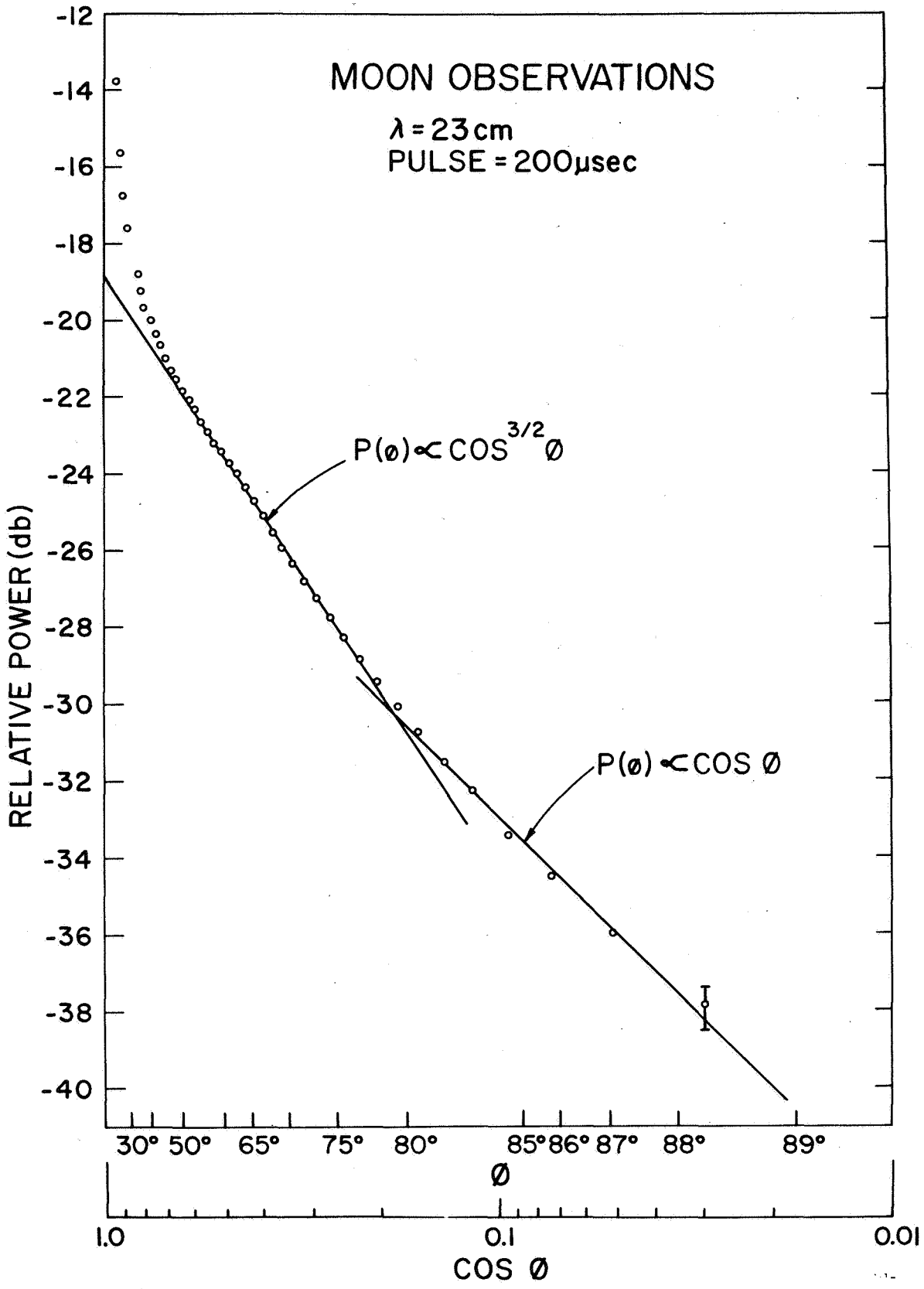
MOON OBSERVATIONS
λ = 23 cm
PULSE = 200 μsec
P(ø) ∝ COS^3/2 Ø
P(ø) ∝ COS Ø
RELATIVE POWER (db)
-12
-14
-16
-18
-20
-22
-24
-26
-28
-30
-32
-34
-36
-38
-40
30° 50° 65° 75° 80° 85° 86° 87° 88° 89°
Ø
1.0
0.1
0.01
COS Ø

Fig. 12

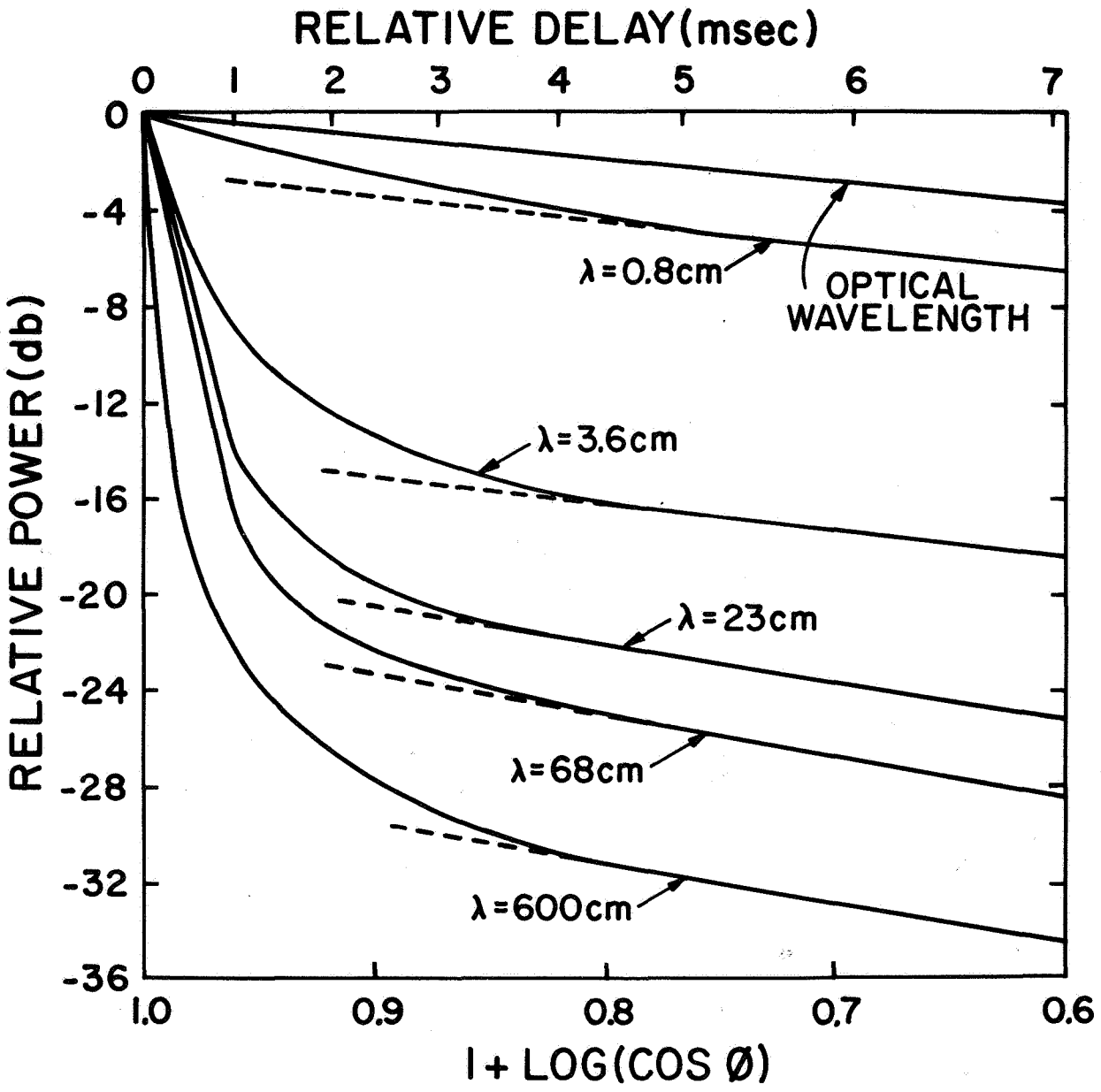
RELATIVE DELAY(msec)
0
1
2
3
4
5
6
7
0
-4
-8
-12
-16
-20
-24
-28
-32
RELATIVE POWER(db)
λ=0.8cm
OPTICAL
WAVELENGTH
λ=3.6cm
λ=23cm
λ=68cm
λ=600cm
1.0
0.9
0.8
0.7
0.6
1+ LOG(COS Ø)

Fig.13

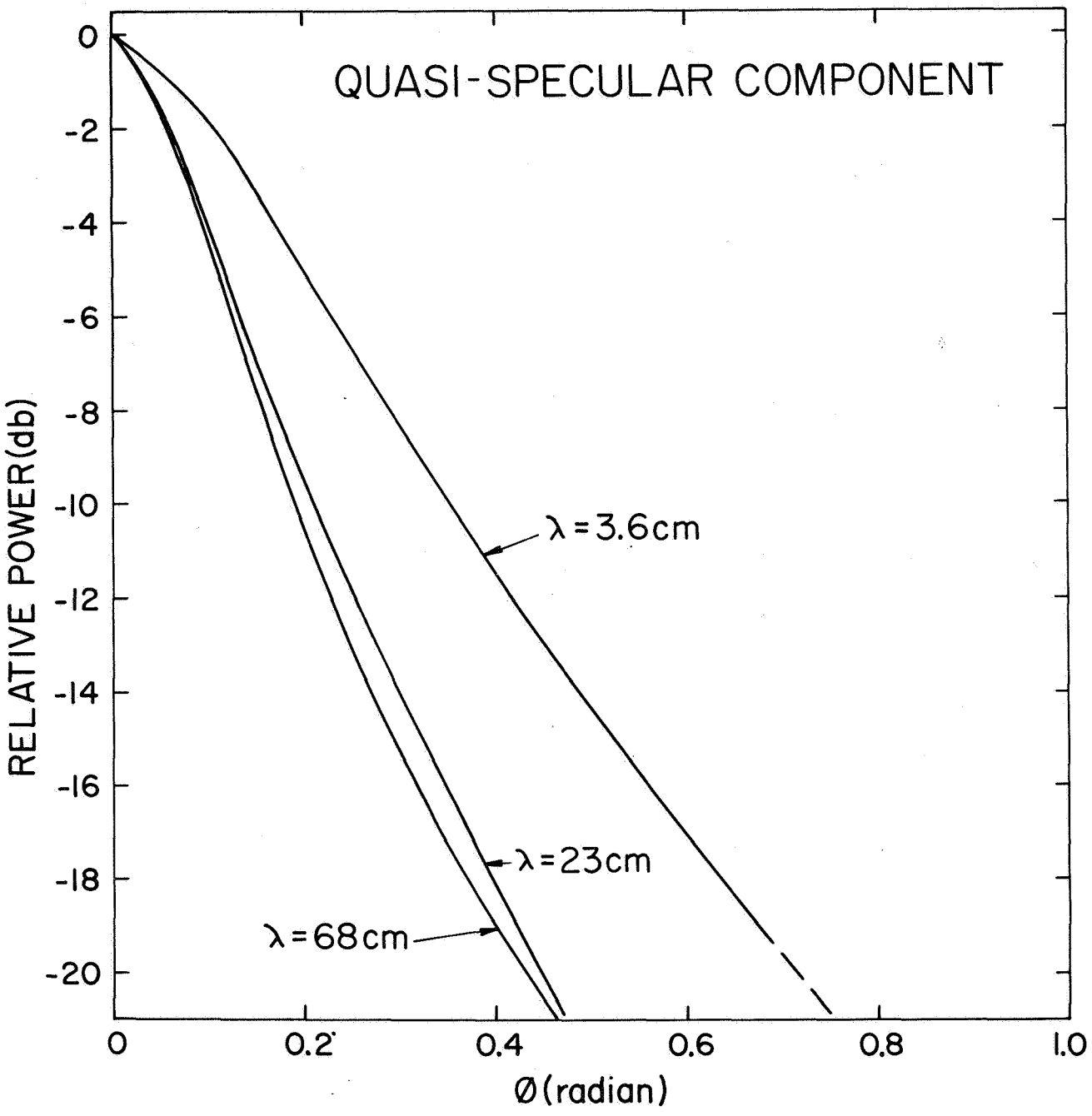
QUASI-SPECULAR COMPONENT
RELATIVE POWER(db)
0
-2
-4
-6
-8
-10
-12
-14
-16
-18
-20
0
0.2
0.4
0.6
0.8
1.0
Ø(radian)
λ=3.6cm
λ=23cm
λ=68cm

Fig. 14

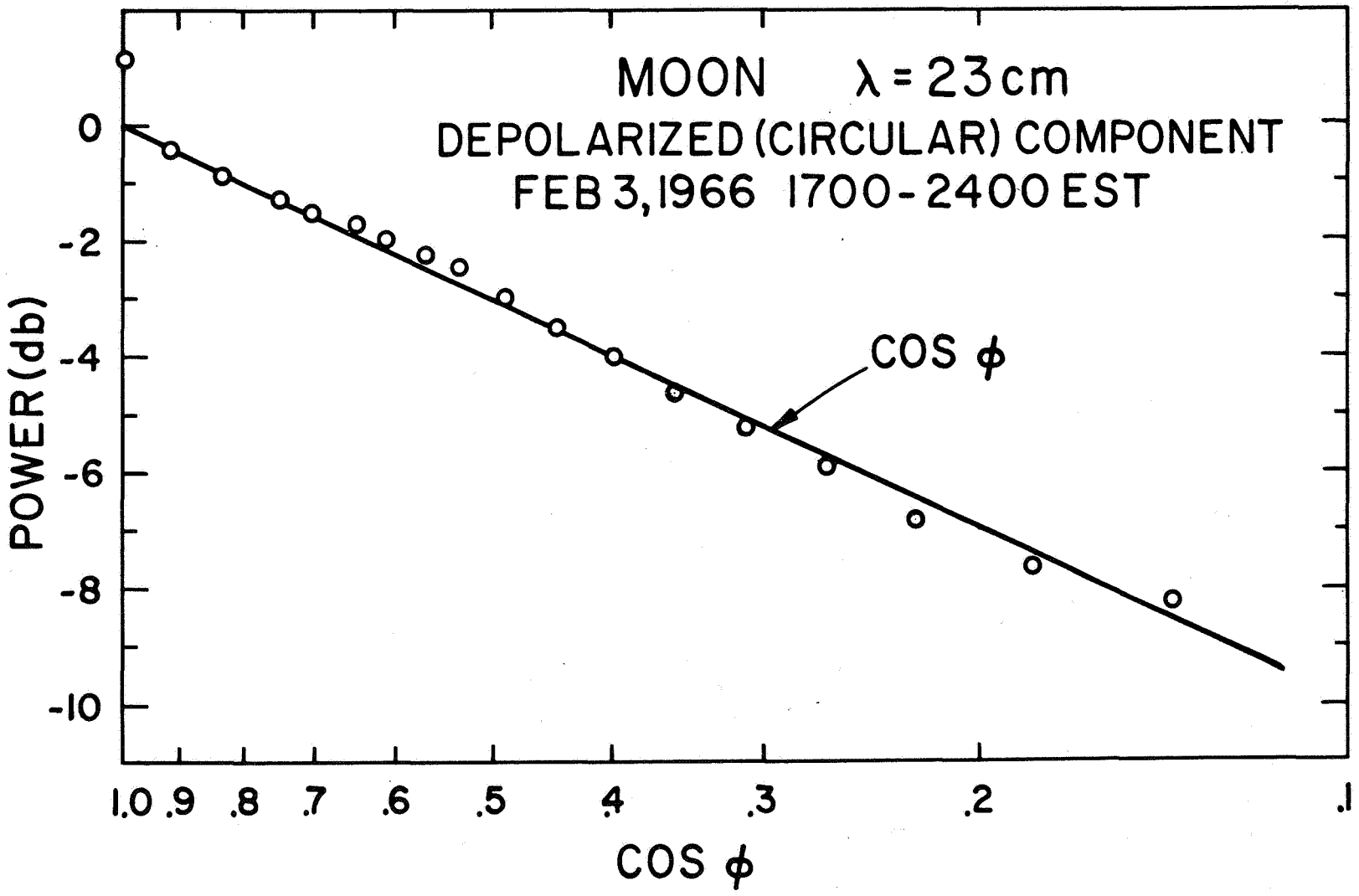
MOON λ = 23cm
DEPOLARIZED (CIRCULAR) COMPONENT
FEB 3, 1966 1700-2400 EST
COS φ
POWER (db)
0
-2
-4
-6
-8
-10
1.0 .9 .8 .7 .6 .5 .4 .3 .2 .1
COS φ
C31-1142

Fig. 15

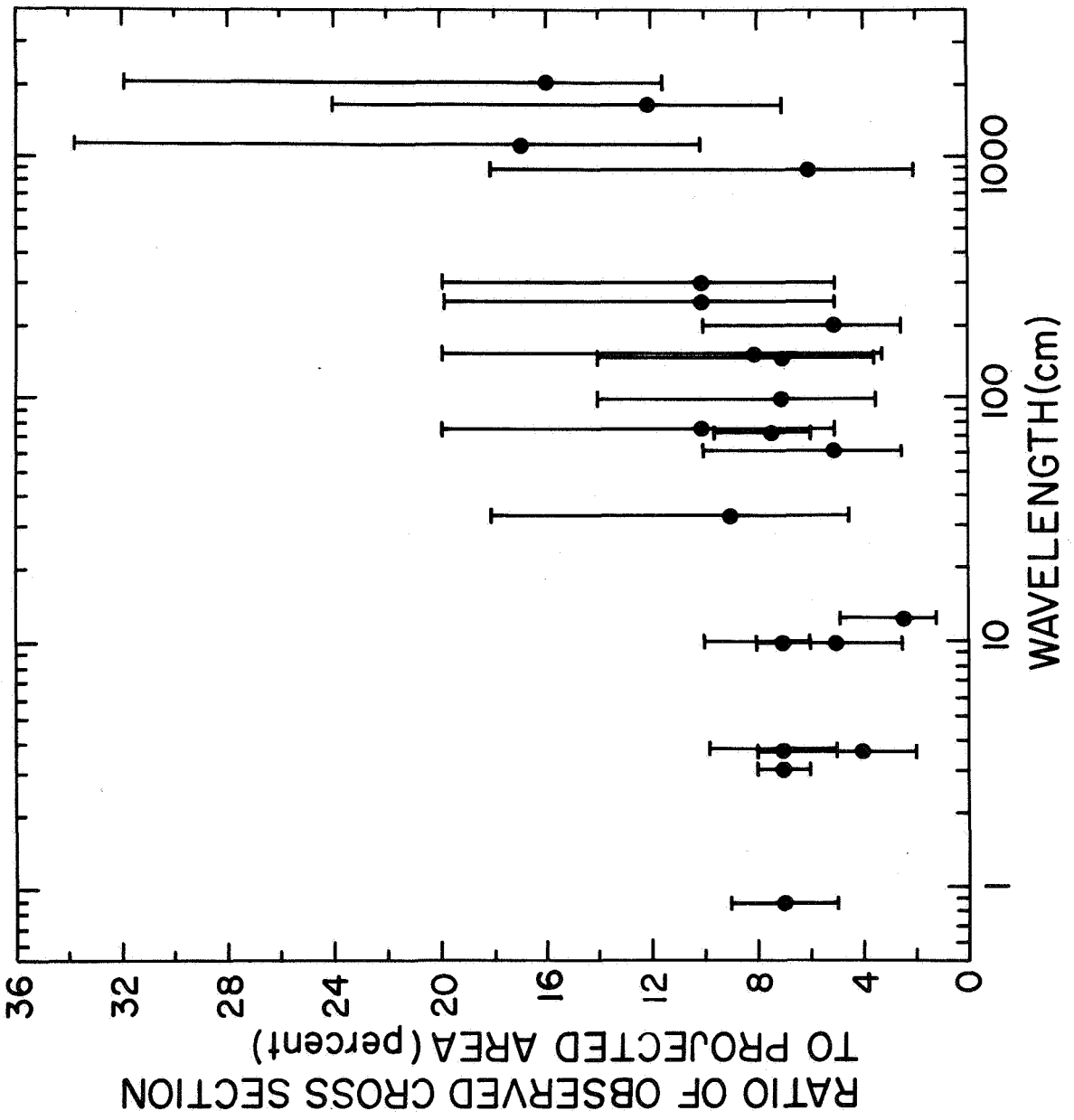
RATIO OF OBSERVED CROSS SECTION
TO PROJECTED AREA (percent)
0
4
8
12
16
20
24
28
32
36
1
10
100
1000
WAVELENGTH(cm)

Fig. 16

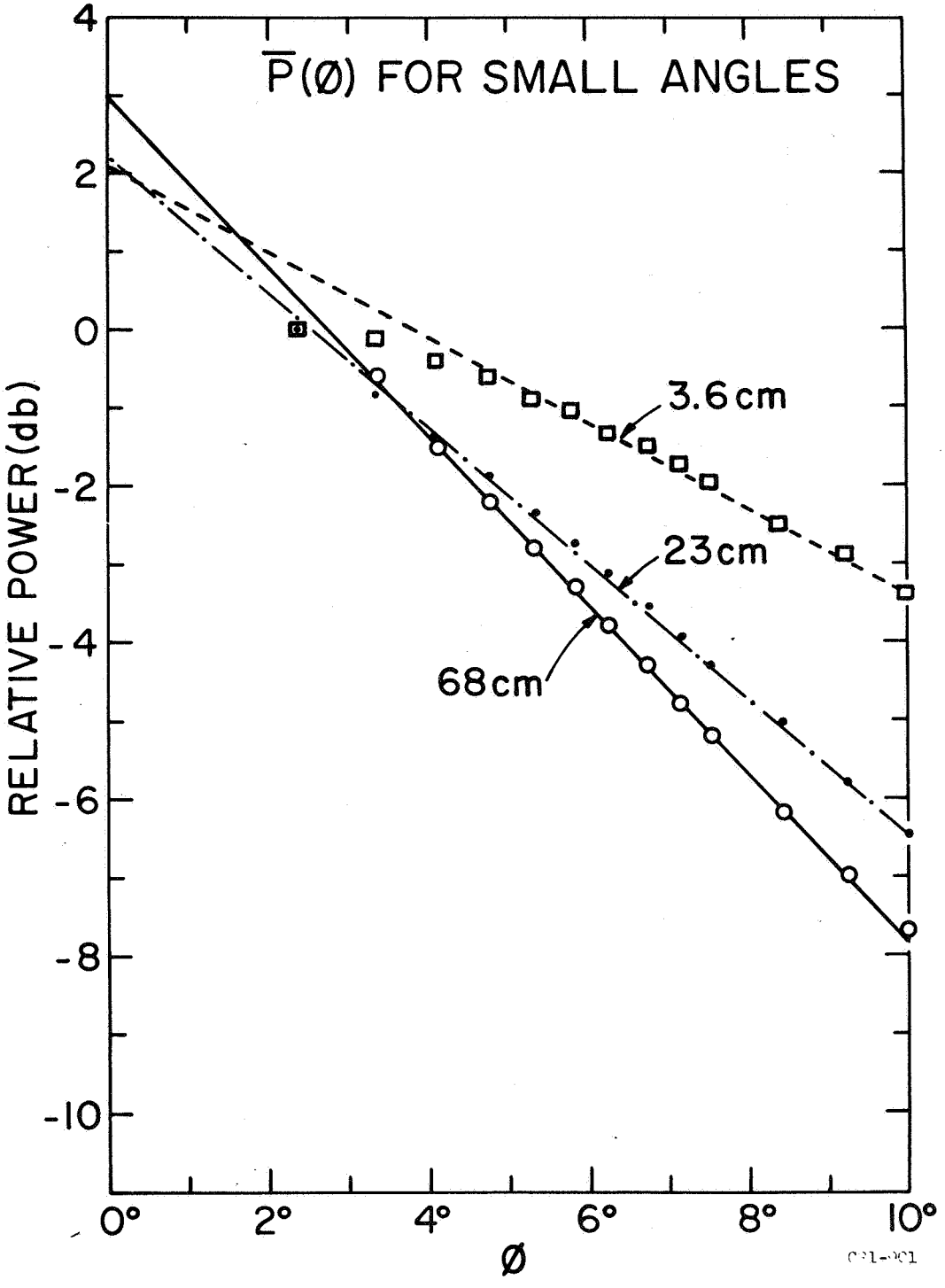
$\overline{P}(\emptyset)$ FOR SMALL ANGLES
RELATIVE POWER (db)
4
2
0
-2
-4
-6
-8
-10
0°
2°
4°
6°
8°
10°
Ø
3.6 cm
23 cm
68 cm

Fig. 17